© 2023. Published by The Company of Biologists Ltd | Development (2023) 150, dev201289. doi:10.1242/dev.201289

RESEARCH ARTICLE

CXCR4 and CXCL12 signaling regulates the development of extrinsic innervation to the colorectum

Viktória Halasy[1], Emőke Szőcs[1], Ádám Soós[1], Tamás Kovács[1], Nóra Pecsenye-Fejszák[1], Ryo Hotta[2], Allan M. Goldstein[2] and Nándor Nagy[1,*]

ABSTRACT

The gastrointestinal tract is innervated by an intrinsic neuronal network, known as the enteric nervous system (ENS), and by extrinsic axons arising from peripheral ganglia. The nerve of Remak (NoR) is an avian-specific sacral neural crest-derived ganglionated structure that extends from the cloaca to the proximal midgut and, similar to the pelvic plexus, provides extrinsic innervation to the distal intestine. The molecular mechanisms controlling extrinsic nerve fiber growth into the gut is unknown. In vertebrates, CXCR4, a cell-surface receptor for the CXCL12 chemokine, regulates migration of neural crest cells and axon pathfinding. We have employed chimeric tissue recombinations and organ culture assays to study the role of CXCR4 and CXCL12 molecules in the development of colorectal innervation. CXCR4 is specifically expressed in nerve fibers arising from the NoR and pelvic plexus, while CXCL12 is localized to the hindgut mesenchyme and enteric ganglia. Overexpression of CXCL12 results in significantly enhanced axonal projections to the gut from the NoR, while CXCR4 inhibition disrupts nerve fiber extension, supporting a previously unreported role for CXCR4 and CXCL12 signaling in extrinsic innervation of the colorectum.

KEY WORDS: Hindgut, Extrinsic innervation, CXCR4, Enteric nervous system, Neural crest cells, Hirschsprung disease

INTRODUCTION

The enteric nervous system (ENS) is the largest subdivision of the peripheral nervous system (PNS), extending from the esophagus to the rectum. Among its many roles is the regulation of gut motility. The ENS consists of two ganglionated plexuses, the myenteric and submucosal plexuses, that are composed of multiple subtypes of neurons and glia arranged in the wall of the bowel in two concentric rings. The enteric neurons of the myenteric and submucosal plexuses form local reflex circuits that, to a large extent, function independently of the central nervous system and regulate the contractility of the bowel wall musculature, as well as the secretion of its glands (Kirchgessner and Gershon, 1990; Schneider et al., 2019). Gut motility disorders are due to congenital absence of enteric neurons, as occurs in Hirschsprung disease, or to degenerative loss of neurons due to infection, inflammation or other causes (e.g. esophageal achalasia and gastroparesis) (Goldstein et al., 2016; Rao and Gershon, 2016; Kang et al., 2021).

The neurons and glia that make up the ENS are derived from multipotent neural crest cells. Neural tube grafting experiments have shown that the cells forming the avian ENS are derived from neural crest cells emigrating from the vagal (somites 1-7) and sacral (caudal to somite 28) levels of the neural tube (Yntema and Hammond, 1954; Le Douarin and Teillet, 1973; Pomeranz et al., 1991; Burns and Le Douarin, 1998; Nagy et al., 2012; Espinosa-Medina et al., 2017; Nagy and Goldstein, 2017). These enteric neural crest-derived cells (ENCCs) migrate and proliferate before differentiating into neuronal and glial subtypes (Young et al., 2005; Nagy et al., 2012). Within the embryonic foregut, vagal neural crest cells migrate in a caudal direction and form the ENS along the entire length of the gastrointestinal tract, whereas sacral neural crest cells enter the cloaca and migrate in an opposing rostral direction, contributing a smaller number of ENS cells primarily to the distal hindgut (Pomeranz et al., 1991; Serbedzija et al., 1991; Burns et al., 2000; Hearn and Newgreen, 2000; Nagy et al., 2007). After gut colonization by ENCCs, extrinsic nerve fibers reach the developing intestinal tract (Teillet, 1978). Recent genetic tracing experiments in mouse embryos demonstrate that Schwann cell precursors invade the hindgut along prevertebral ganglia- and pelvic ganglia-derived extrinsic nerves, adopting first an enteric glial phenotype and subsequently differentiating into primarily calretinin-expressing neurons (Uesaka et al., 2015; Niu et al., 2020).

In the avian embryo, sacral neural crest cells migrate out of the neural tube on day 3 of embryonic development and colonize the cloaca 48 h later (Pomeranz et al., 1991; Serbedzija et al., 1991; Nagy et al., 2007), a process that in mouse embryos occurs between embryonic days 9.5 and 11.5 (Wang et al., 2011). In birds, the sacral crest-derived nerve of Remak (NoR), which is an autonomic ganglionated chain located in the dorsal mesentery from the upper third of the midgut to the cloaca, contributes to the extrinsic innervation of the colorectum (Teillet, 1978; Suzuki et al., 1996). The avian pelvic plexus, similar to mouse pelvic ganglia, also provides a source of extrinsic fibers to the distal hindgut (Nolf, 1934; Nagy et al., 2007).

Despite the progress made in the characterization of morphogens, transcription factors and cell adhesion molecules involved in ontogeny of the ENS, very little is known about the developmental mechanism of extrinsic innervation of the hindgut. In chicken, neuropilin 1 mRNA, which is expressed by the NoR at E6 and E8, and its ligand, semaphorin D (also known as collapsin 1) (which is expressed in the hindgut mesenchyme), provoke mucosal chemorepulsion of extrinsic nerve fibers (Shepherd and Raper, 1999). *PROX1*, a homeodomain transcription factor, is expressed in the NoR before its fibers penetrate into the colon (Margarido et al., 2020), suggesting a potential role for this protein in sacral neural crest cell specification.

[1]Department of Anatomy, Histology and Embryology, Faculty of Medicine, Semmelweis University, Budapest 1094, Hungary. [2]Department of Pediatric Surgery, Pediatric Surgery Research Laboratories, Massachusetts General Hospital, Harvard Medical School, Boston, MA 02114, USA.

*Author for correspondence (nagy.nandor@med.semmelweis-univ.hu)

V.H., 0000-0002-1713-5986; Á.S., 0000-0002-1660-3303; N.N., 0000-0002-6223-5214

Handling Editor: Patrick Tam
Received 9 September 2022; Accepted 25 January 2023

Development (2023) 150, dev201289. doi:10.1242/dev.201289

CXCR4 signaling has an important role in neurogenesis by supporting the migration, proliferation and differentiation of neural progenitor cells, and by influencing neural crest cell migration and neuronal axonal projection (Doitsidou et al., 2002; Lieberam et al., 2005; Belmadani et al., 2005; Tanaka et al., 2010; Cheng et al., 2017). Recent work with chicken embryos has shown that CXCR4-expressing cardiac neural crest cells migrate toward the chemokine CXCL12 (also named SDF-1) produced by the pharyngeal arches. Disrupting CXCL12 and/or CXCR4 signaling causes abnormal migration of cardiac neural crest cells (Escot et al., 2013; Tang et al., 2021). Other subsets of cranial and trunk neural crest cells destined to form sympathetic ganglia also express CXCR4 and migrate in response to CXCL12 (Olesnicky Killian et al., 2009; Kasemeier-Kulesa et al., 2010). However, its expression in the gastrointestinal tract has not been studied.

We observed that in the developing mammalian and avian embryo, CXCR4 is specifically expressed by the pelvic plexus and NoR, suggesting a role for CXCR4-CXCL12 signaling in development of sacral crest-derived derivatives. We therefore examined the role of CXCL12 in regulating extrinsic innervation in the chick hindgut. Using avian embryo manipulations combined with organ cultures, we provide experimental evidence that CXCR4 and CXCL12 signaling regulate nerve fiber growth during extrinsic innervation of the colorectum by the NoR.

RESULTS

CXCR4 is expressed by chicken vagal, but not sacral, neural crest cells

Although CXCR4 is known to be expressed in the avian cranial and cardiac neural crest (Rezzoug et al., 2011; Escot et al., 2013), a detailed analysis of its expression during trunk neural crest cell development has not been described. To characterize the spatiotemporal expression pattern of CXCR4 receptor in the trunk region of chick embryos at the onset of neural crest cell (NCC) migration, immunofluorescence staining was performed at Hamburger-Hamilton (HH) stage 13 (embryonic day 2; E2) through HH20 (E3). Coronal and cross-sections of HH13 chicken embryo were immunostained using anti-CXCR4 monoclonal antibody (Escot et al., 2013; Nagy et al., 2020). Coronal sections through the cervical somites demonstrate that CXCR4 is specifically expressed in the streams of migrating vagal crest crest-derived cells identified by the marker SOX10 (Fig. 1A-A‴,B). In consecutive cross-sections of the 1st to 3rd somite level, strong CXCR4 immunoreactivity was found in the cardiac neural crest positioned in the mesenchyme of the pharyngeal arches (Fig. 1C-C″). CXCR4 was prominent on NCCs at the somite level, but its expression decreased as crest cells progressed ventrally toward the pharyngeal arches and foregut. To quantify the relative levels of CXCR4 expression, the mean fluorescent intensity across vagal crest cells was measured according to Shihan et al. (2021). The quantified mean gray value based on the CXCR4 fluorescence in vagal NCCs (n=20) located at somite levels 1-3 (cardiac crest cells) was significantly higher (101.7±6.726) than in the posterior vagal crest region (somite level 4 to 7) (61.59±2.614) (Fig. 1B). Caudal to the vagal crest region, no CXCR4 expression was found in the delaminating SOX10$^+$ trunk or sacral neural crest cells (Fig. 1D-F). Thus, CXCR4 was expressed on the vagal crest cells, although its expression was also observed in several other cell types, including intersomitic vascular endothelial cells (Fig. 1A″) and neural tube (Fig. 1C-F), as previously reported (Tachibana et al., 1998; McGrath et al., 1999; Yusuf et al., 2005; Chen et al., 2007; Kasemeier-Kulesa et al., 2010).

CXCR4 is expressed by the sacral crest-derived nerve of Remak

At later developmental stages, CXCR4 expression was also reported on trunk neural crest-derived sympathetic ganglia and dorsal sensory ganglia (Yusuf et al., 2005; Rezzoug et al., 2011; Yahya et al., 2021), but a detailed analysis of its expression during developing chicken and mammalian ENS has not been described. To determine the spatiotemporal expression of CXCR4 in the hindgut region of chicken embryo during neural crest cell colonization and differentiation, we combined CXCR4 immunocytochemistry with ENCC-specific P75^{NTR}, enteric neuron specific CN monoclonal antibody, anti-HU (ELAV-like protein 4), anti-TUJ1 (TUBB3) and enteric glia specific brain-fatty acid binding protein (BFABP; FABP7) immunostaining. In chicken embryo at 5-day embryonic age (E5, Hamburger-Hamilton stage 27; HH27), vagal crest-derived ENCCs colonize the foregut and midgut part of the embryonic intestine. At this stage, sacral crest-derived cells reach the dorsal mesentery and give rise to the NoR (Nagy et al., 2007). ENCCs traveling in a craniocaudal direction arrive in the area of the distal cecum at E6 (HH28; Fig. 2A) and, over the next 3 days, migrate through the hindgut into the proximal cloaca (Fig. 2C). Beginning at E6, CXCR4 expression was observed throughout the P75$^+$ NoR (Fig. 2B-B″). At E9 (HH35) and E12 (HH38), CXCR4 continues to be expressed by the NoR and its nerve fibers projecting to the gut (Fig. 2D′,G′). CXCR4 is not expressed by the HU$^+$/CN$^+$ enteric neurons (Fig. 2E′,G′) or E6 vagus nerve (data not shown). By E14 (HH40), reduced CXCR4 immunoreactivity was observed in the NoR, being retained mainly in endothelial cells of larger vessels (Fig. 2I-I″). Analysis of CXCR4 expression in the developing chick colon using neuron- and glia-specific antibodies showed that CXCR4 colocalized with CN$^+$ neural cells in the NoR and its nerve fibers (Fig. 3A-A″), and not with BFABP$^+$ glial cells (Fig. 3B-B″).

The Nerve of Remak contributes nerve fibers to the hindgut mesenchyme and ENS

To determine the relationship between NoR and hindgut ENS, we removed the NoR at E6 and replaced it with a new NoR harvested from age-matched green fluorescent protein (GFP)-expressing chick embryos (chick^{GFP}). HU$^+$ ganglion cells originating from the SOX10$^+$ ENCCs are present in the mesenchymal layer of the ceca and proximal hindgut at this stage (Nagy et al., 2021; Fig. 4A, schematic illustration). These chimeric hindgut recombinants were cultured overnight in 3D collagen gel and then grown on the chorioallantoic membrane (CAM) of a host chicken embryo for an additional 7 days (Fig. 4A,B). As shown in Fig. 4B-D, the CAM graft became completely colonized by host ENCCs that differentiated to normal-appearing ENS. Many GFP$^+$ fibers are present in the CAM grafts (Fig. 4C), demonstrating that nerve fibers originating from the GFP-expressing chick NoR are capable of penetrating into the chick hindgut in these chick–chick^{GFP} tissue recombinants and innervate the enteric ganglia (Fig. 4C). The percentage contribution of intrinsic versus extrinsic nerve fiber origin showed that TUJ1 immunoreactivity had a significantly higher positive rate in GFP-negative nerve fibers (68.03±9.00%) compared with GFP$^+$ nerve fibers (31.96±9.00%) (Fig. 4D). To confirm the contribution of nerve fibers from NoR to hindgut in the presence of vagal crest-derived ENCCs, E1.5 (HH10) vagal neural tube and its associated neural crest from GFP chicken embryos were grafted into age-matched wild-type chicken embryos (Fig. 4E) and incubated for an additional 8 days. GFP immunostained vagal crest-derived ENCCs are seen in the enteric plexuses of the gut wall (Fig. 4F,G), similar to those seen in our previous work (Nagy et al., 2012; Delalande et al., 2021).

Development (2023) 150, dev201289. doi:10.1242/dev.201289

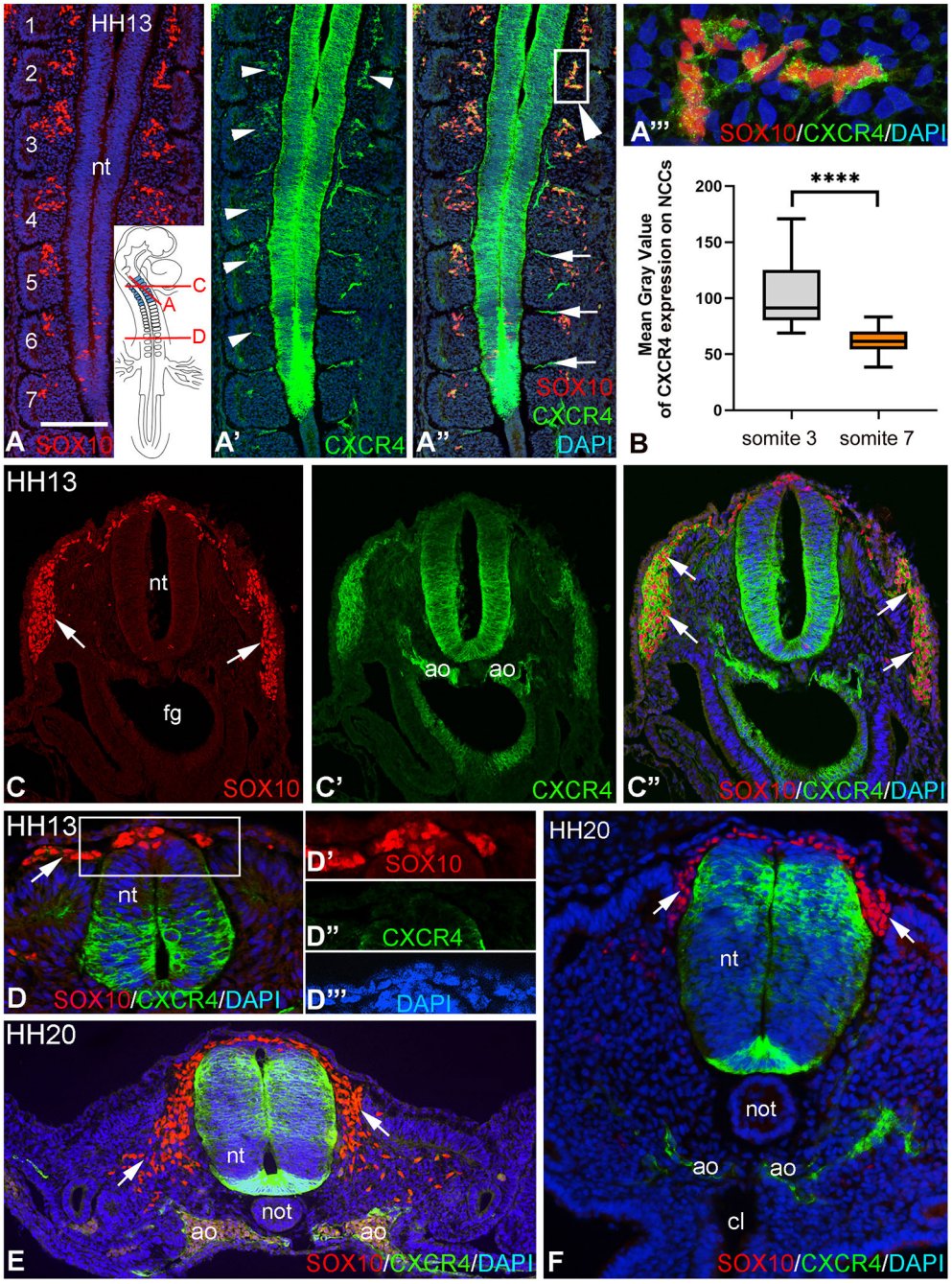

Fig. 1. CXCR4 is expressed by vagal, but not sacral, neural crest cells during chick development. (A-F) CXCR4 immunofluorescence at Hamburger-Hamilton stage (HH) 13 (A-D‴) and HH20 (E,F) chick embryos. (A-A‴) SOX10 and CXCR4 expression patterns during vagal NCC migration. Coronal sections through vagal level of HH13 chick embryo. SOX10$^+$ vagal NCCs migrate through the anterior half of the somites and express CXCR4. Numbers indicate the first eight formed somites and arrowheads indicate CXCR4 expression. CXCR4$^+$ intersomitic blood vessels (A″, arrows) do not express SOX10. (A‴) A magnified view of A″ shows SOX10$^+$/CXCR4$^+$ vagal NCCs. (B) Quantification of mean intensity value in the particle expressed in gray-level units of SOX10$^+$/CXCR4$^+$ immunoreactive cells. (C-F) Cross-sections at the level of developing heart (C-C″), trunk (D,E) and cloaca (F). SOX10$^+$ vagal neural crest cells express the CXCR4 receptor (arrows, C-C″), but trunk neural crest cells (D,E) and sacral neural crest cells (F) do not (arrows). (D′-D‴) Magnified views from D showing SOX10$^+$/CXCR4$^-$ trunk NCCs. A Mann–Whitney U-test was used for B. ****P<0.0001. Data are mean±min and max value; error bars indicate s.e.m. Scale bar: 170 µm (A-A″); 15 µm (A‴); 90 µm (C-C″); 40 µm (D); 30 µm (D′-D‴); 120 µm (E); 60 µm (F). ao, aorta; cl, cloaca; not, notochord; nt, neural tube.

TUJ1$^+$/GFP-negative nerve projections are present in the hindgut along with GFP$^+$ enteric ganglia. Some TUJ1$^+$ nerve fibers may be of extrinsic origin from the GFP-negative NoR and some may come from GFP-expressing ENCCs (TUJ1$^+$/GFP$^+$) in the hindgut that have differentiated to give rise to enteric ganglia (Fig. 4G-G″). These results demonstrate that the NoR sends numerous nerve fibers into the intestinal wall and also contributes to the extrinsic innervation of the hindgut ENS.

Pelvic ganglia in embryonic avians and mammals express CXCR4

Sacral-derived NCCs form the pelvic plexus in avian (Yntema and Hammond, 1954; Catala et al., 1995; Nagy et al., 2012) and mammalian embryos (Kapur, 2000). We hypothesized that, similar to NoR, the pelvic plexus (Nagy et al., 2012) should express the CXCR4 receptor. To assess CXCR4 expression during development of the pelvic ganglia, we performed double immunocytochemistry on multiple cross-sections of E8 chicken embryo at the level of the tail bud (Fig. 5A). The pelvic ganglia appear as paired structures surrounding the cloaca. Immunofluorescence showed that, at E9, CXCR4$^+$ cells were present in the sacral neural crest-derived P75$^+$ pelvic plexus (Fig. 5B-B″). To characterize the immunophenotype of the P75$^+$ cells further, double-immunostaining was performed. HU immunohistochemistry showed the presence of large number of neurons in the P75$^+$ pelvic ganglia (Fig. S1A-B″). The pelvic ganglia also express neurofilament (Fig. S1C-D″), but not neuronal nitric oxide synthase (nNOS; Fig. S1E-F″). However, differentiated nNOS immunoreactive neurons are present in the hindgut myenteric

Development (2023) 150, dev201289. doi:10.1242/dev.201289

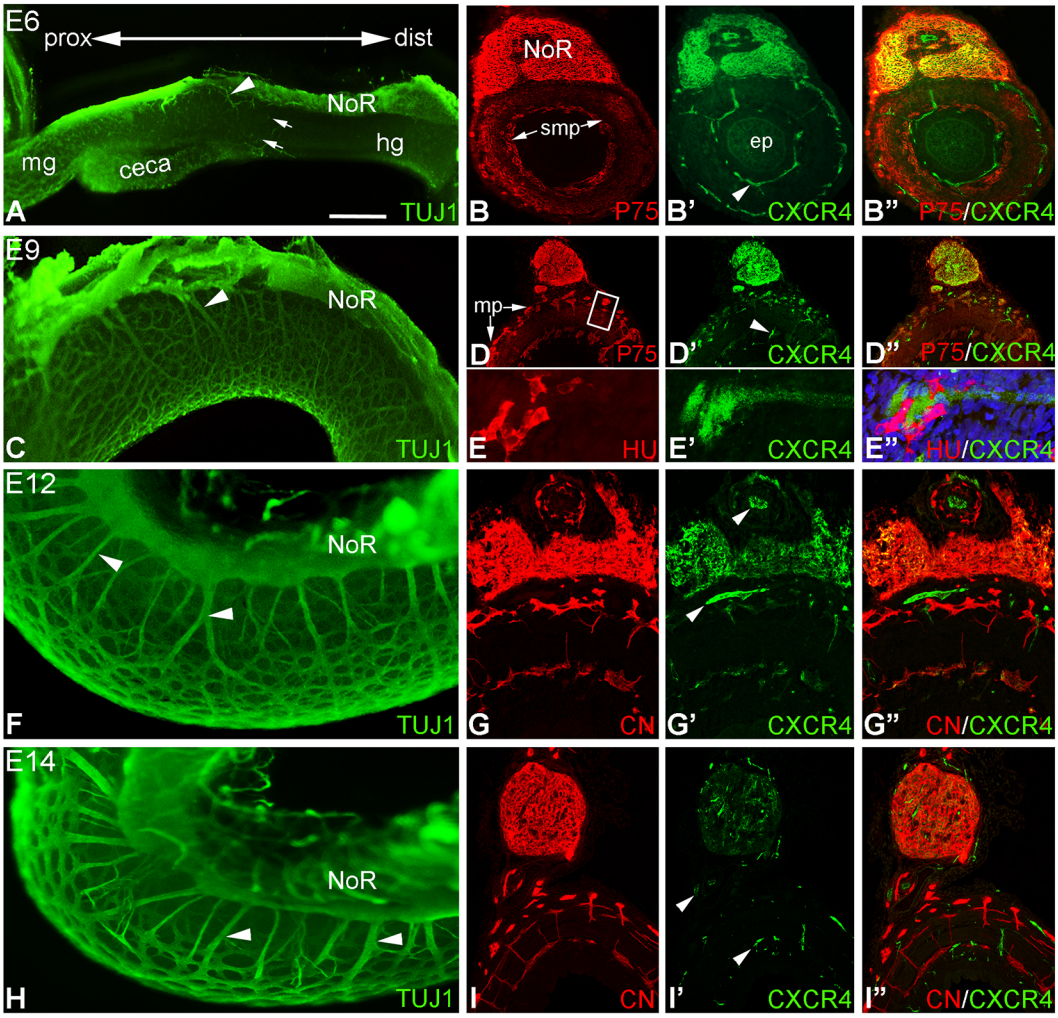

Fig. 2. CXCR4 is expressed by the NoR, but not by the intrinsic ENS. (A,C,F,H) TUJ1 whole-mount immunostaining of E6 (A), E9 (C), E12 (F) and E14 (H) chick hindgut shows the developing NoR and its extrinsic fibers (arrowheads) projecting to the gut wall. At E6 (A), the NoR forms in the dorsal mesentery adjacent to the distal gut. At this stage, the vagal crest-derived ENCC wavefront has reached the proximal hindgut (arrows). Sections of E6 (B-B″), E9 (D-E″), E12 (G-G″) and E14 (I-I″) chicken hindgut show that the intrinsic and extrinsic neural elements are labeled with NCC-specific P75 and neuron-specific CN and HU antibodies. (E-E″) Higher magnifications of D-D″. The CXCR4 receptor is expressed by the NoR and blood vessels (arrowheads), but not by intrinsic ENS (right column). Myenteric plexuses are innervated by CXCR4$^+$ NoR (E-E″). CXCR4 expression in NoR increases until E12 (B′,D′,E′) then declines significantly (G′,I′). Scale bars: 400 µm (A), 130 µm (B-B″), 180 µm (C), 200 µm (D-D″), 25 µm (E-E″), 230 µm (F), 100 µm (G-G″), 340 µm (H), 200 µm (I-I″). dist, distal; ep, epithelium; hg, hindgut; mg, midgut; mp, myenteric plexus; NoR, nerve of Remak; prox, proximal; smp, submucosal plexus.

plexus (Fig. S1G-G‴). We extended our analysis to pelvic ganglia of mouse and human embryos. Using lineage-tracking in *Wnt1:Cre/mTmG* transgenic mice, we followed the contributions of ENCCs to hindgut innervation. During ENS development, GFP-labeled ENCCs migrated into the mouse distal hindgut at E13.5 and, ultimately, differentiated into the myenteric ganglia in the outer layer of the hindgut. At this stage the pelvic ganglia develop as paired structures between the hindgut and the urinary bladder (Fig. 5C,D), and express CXCR4 (Fig. 5D′,D″). The vagal crest-derived ENCCs in the myenteric plexus (Fig. 5E) were CXCR4 negative (Fig. 5E′,E″). A similar picture was obtained when examining the human embryo (Fig. 5F-H″). HNK1, a marker specific to neural crest cells, outlines the pelvic ganglia at the level of the hindgut and bladder (Fig. 5F,G), and these cells carry the CXCR4 receptor on their surface (Fig. 5G′,G″). In contrast, intrinsic elements of the ENS are negative for CXCR4 (Fig. 5H-H″). Similar to chicken embryo, CXCR4 also marks the mammalian endothelial cells of larger blood vessels (arrowheads in Fig. 5B′,D′,E′,G′,H′).

Expression of *CXCR4* and its ligand, *CXCL12*, in the chicken embryo

The spatiotemporal expression of *CXCR4* and *CXCL12* in the developing hindgut and cloacal region was examined by *in situ* hybridization. In E6 chick embryos, *CXCR4* transcripts were found in the ventricular layer of the neural tube and in the NoR of the hindgut (Fig. 6A-A″). As development proceeds, the location and distribution of the *CXCR4*-expressing cells were found in the P75$^+$ NoR (Fig. 6B-B″) and P75$^+$ ganglia of the pelvic plexus (Fig. 6C-C″). Serial sagittal sections from an E10 chicken embryo tail bud revealed the ganglia of the pelvic plexus and the NoR at the level of the proctodeum and the bursa of Fabricius (Fig. 6C). *CXCR4* expression was not observed in ENCCs during their migration to the hindgut (Fig. 6B″). To determine whether *CXCL12* (the ligand for *CXCR4*) signaling correlates with NoR development and may constitute a guidance cue for the NoR-derived nerve fibers, we examined the expression of *CXCL12* during hindgut development. In E6 chick embryo, *CXCL12* is highly expressed in mesenchymal

Development (2023) 150, dev201289. doi:10.1242/dev.201289

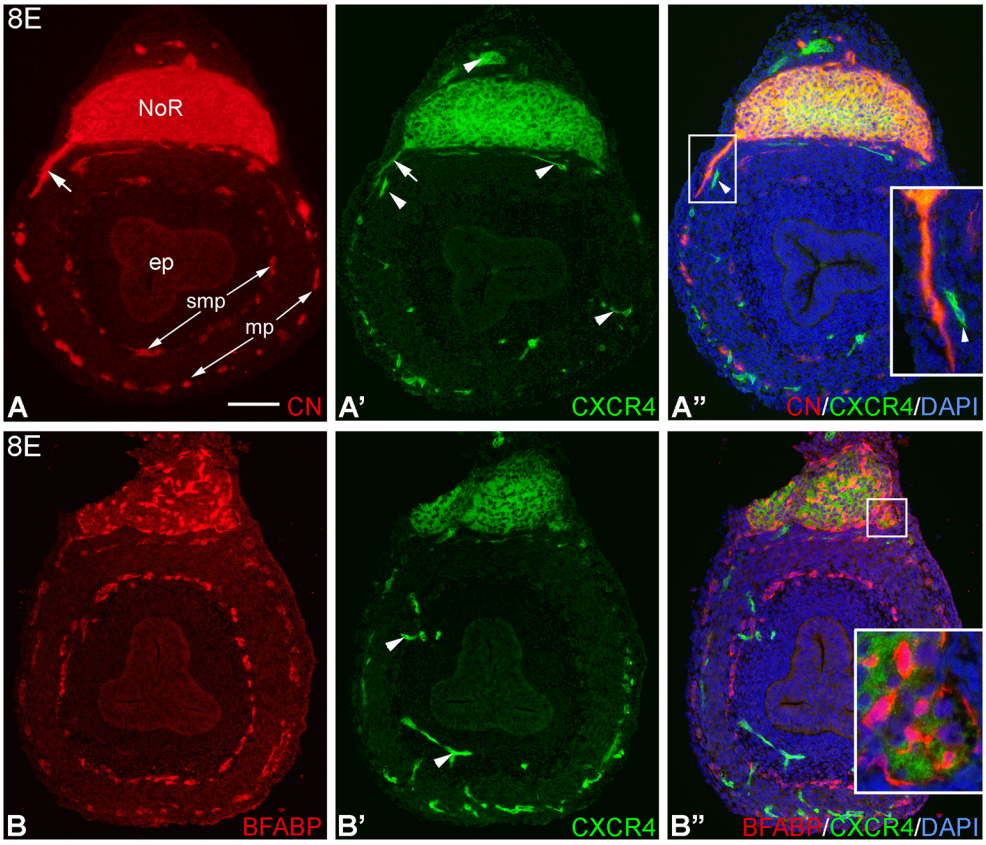

Fig. 3. Nerve of Remak neurons express CXCR4. (A-A″) Both intrinsic and extrinsic neurons of the E8 chicken hindgut show CN immunoreactivity. Arrows indicate extrinsic fibers of nerve of Remak (NoR) origin. Inset: double immunofluorescence staining shows that CN^+ axons strongly express CXCR4. Arrowhead marks the $TUJ1^-/CXCR4^+$ blood vessels. (B-B″) $BFABP^+$ glial cells do not co-express CXCR4. Arrowheads indicate $CXCR4^+$ blood vessels. Outlined area in B″ is magnified in the inset, demonstrating no overlap between $CXCR4^+$ cells and $BFABP^+$ glial cells. Scale bar: 100 µm (A-A″); 50 µm (A″, inset); 100 µm (B-B″); 20 µm (B″, inset). ep, hindgut epithelium; mp, myenteric plexus; NoR, nerve of Remak; smp, submucosal plexus.

cells surrounding the NoR in the mesentery, but not in visceral smooth muscle cells of the hindgut (Fig. 7A-A″). It is noteworthy that although *CXCR4* and *CXCL12* were prominent in the NoR region, *CXCL12* expression was also found in other parts of the developing hindgut, including the gut epithelium (Fig. 7B,C) and muscularis externa (Fig. 7B). In later embryonic stages (at E14), *CXCL12* expression decreased gradually in the mesenchyme surrounding the NoR and shifted to the enteric ganglia (Fig. 7C, inset). These results show that *CXCR4* signaling in NoR and hindgut is complementary with *CXCL12* expression and appears to be linked to the formation of extrinsic innervation of the hindgut.

Exogenous CXCL12 promotes neurite outgrowth from NoR *in vitro*

Recent studies in rodents have suggested that CXCL12 is involved in axonal pathfinding, outgrowth and branching (Bhardwaj et al., 2013; Hilla et al., 2021). To test this in the avian NoR and ENS, we cultured E6 chicken midgut, ceca and hindgut on a fibronectin-coated surface for 24 h in the absence (DMEM, Fig. 8A) or presence of recombinant CXCL12 protein (Fig. 8B). Addition of 100 ng/ml Cxcl12 to the culture medium resulted in robust neurite outgrowth from the NoR (Fig. 8B). As shown in Fig. S2, the presence of CXCL12 did not promote ENCC migration from the midgut and ceca, whereas addition of GDNF (10 ng/ml) induced robust ENCC migration. Hindgut treated with 200 µM AMD3100, a CXCL12 antagonist, alone or in combination with 100 ng/ml CXCL12, led to inhibition of neuronal extension from the NoR (Fig. 8C). Quantification of the neuronal extension from the NoR and migration of NCCs was analyzed with TUJ1 and SOX10 specific immunostaining in the CXCL12 and AMD3100 treated cultures, with four or five data points measured from each hindgut (n=5 guts per group). The CXCL12 treatment induced significantly greater NoR-derived neuronal projections on the fibronectin-coated surface (Fig. 8B). The average distance of the $TUJ1^+$ fibers was 876.50 ±57.09 µm from the explant, when compared with the lengths of the control-treated (DMEM, 284.10±23.41 µm) and AMD3100-treated hindgut fibers (319.50±17.99 µm) (Fig. 8D). We selected two 300×900 µm sized stripes per gut perpendicular to the NoR and counted all the emigrated $SOX10^+$ cells. CXCL12 treatment resulted in significantly more migrated NCCs (127.7±17.33), whereas this was reversed in control- (43.66±6.878) and AMD3100- (51.7±6.723) treated explants (Fig. 8E). $SOX10^+$ cells that emigrated from the NoR were always associated with extending $TUJ1^+$ neurites (Fig. 8B, insets).

Inhibition of CXCR4 signaling disrupts extrinsic innervation of the gut

To investigate the role of CXCR4 and CXCL12 signaling during development of hindgut extrinsic innervation, we examined the development of TUJ1-expressing nerve fibers in hindgut explants. E6 chick gut, including ceca and hindgut, was cultured for 3 days with or without addition of AMD3100 (n=5/culture condition). Similar to E9 chicken hindgut (Fig. 9A), in normal culture media conditions, ENS colonization of the hindgut was completed and $TUJ1^+$ NoR-derived extrinsic nerve fibers penetrated the wall of the hindgut (Fig. 9B, arrows). Addition of AMD3100 to the media did not interfere with ENCC migration (Fig. 9C), but did inhibit nerve fiber extension from the NoR, as shown by the absence of TUJ1-expressing fibers (Fig. 9C). For statistical analysis, the nerve fiber properties (number, length and thickness) of TUJ1 whole-mount immunostaining were measured in each group. There are significant differences between number, length and thickness of NoR fibers:

Development (2023) 150, dev201289. doi:10.1242/dev.201289

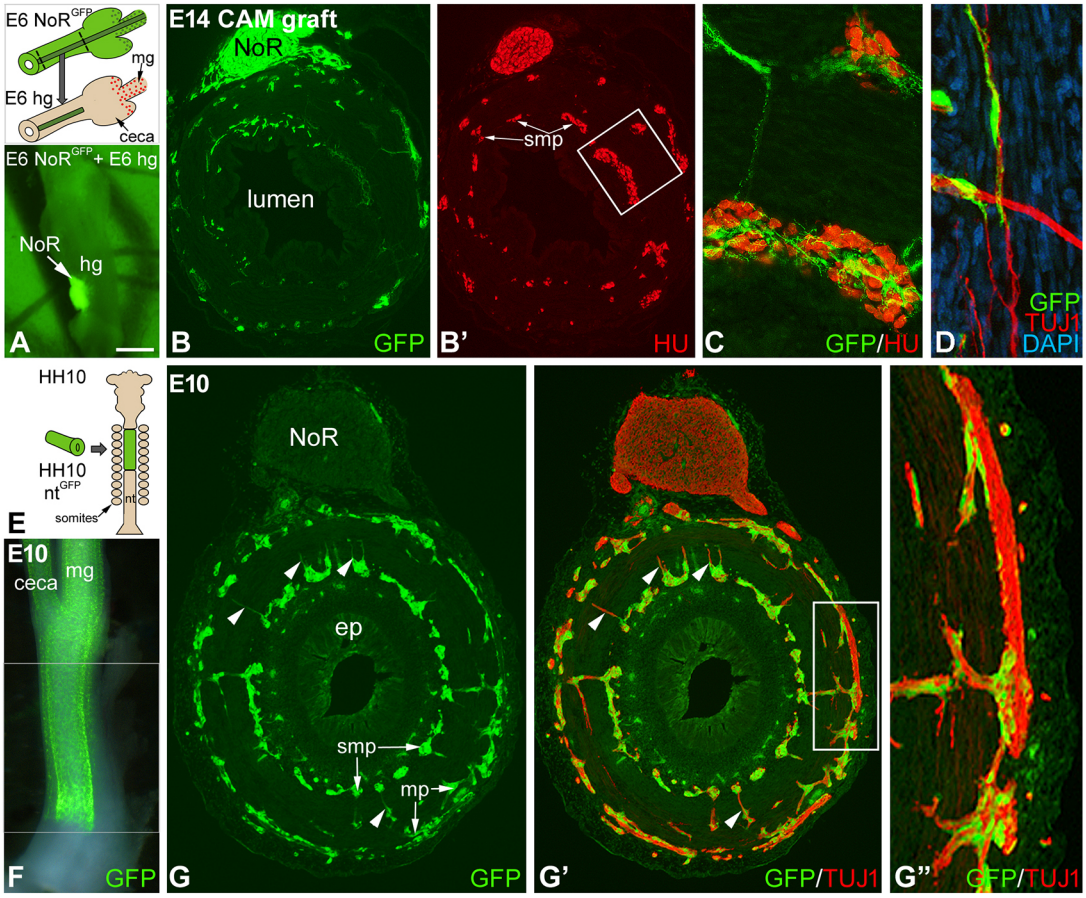

Fig. 4. Fibers originating from the NoR innervate the enteric ganglia. (A-C) Chick-chick^{GFP} chimera demonstrate that the nerve of Remak (NoR) contributes nerve fibers to the hindgut ENS. (A) Schematic illustration of tissue recombinations of E6 chick^{GFP} NoR and E6 chick midgut-hindgut cultured overnight in 3D-collagen gel and then transplanted onto a chorioallantoic membrane (CAM). Red dots show that, at the time of recombination, the midgut and ceca already contain vagal-derived ENCCs. (B) After 7 days of CAM culture, chick^{GFP} NoR-derived fibers enter the hindgut. (C) GFP-expressing NoR fibers and terminals with a basket-like shape are found within the enteric ganglia and associate with the HU^{+} neurons. Outlined area in B′ is magnified in C. To determine whether any neurofibers originate from the NoR, sections were double immunostained using anti-GFP and TUJ1 antibodies, showing that many TUJ1^{+} fibers arising from the chick^{GFP} NoR are connected to the TUJ1^{+}/GFP^{-} intrinsic plexuses (D). (E-G″) Transplantation of a GFP^{+} neural tube into a wild-type chicken at E1.5 and further incubation for 8 days. The schematic illustration shows the microsurgical removal of the HH10 neural tube at the level of somites 2-7 and recombination with equivalent tissue obtained from age-matched chick^{GFP} embryo. Whole-mount GFP immunostaining (F) and cross-sections (G-G′) of E10 hindgut immunolabeled with TUJ1 shows that at this developmental stage, GFP^{+} vagal neural crest cells have colonized the entire colorectum. Neither the TUJ1^{+} NoR nor the extrinsic fibers express GFP. Area outlined in G′ is magnified in G″, where the TUJ1/GFP-negative extrinsic fibers reach the TUJ1^{+}/GFP^{+} intrinsic plexuses (arrowheads in G,G′). Scale bar: 400 µm (A); 170 µm (B,B′); 40 µm (C,D); 600 µm (F); 100 µm (G,G′); 35 µm (G″). ep, hindgut epithelium; hg, hindgut; mg, midgut; NoR, nerve of Remak; mp, myenteric plexus; nt, neural tube; smp, submucosal plexus.

the average number of E9 hindgut TUJ1^{+} nerve fibers (12.00 ±0.8367) is significantly higher compared with hindguts treated with the AMD3100 inhibitor (7.00±0.8944), but not in control DMEM cultures (10.00±0.4082). The average length of fibers projecting from the NoR to the hindgut wall was significantly reduced in the AMD-treated group (179.1±28.06 µm) when compared with the E6+72 h DMEM (403.2±26.77 µm) and E9 (499.2±29.32 µm) hindguts. These shorter fibers were also significantly thinner (8.899±0.8527 µm) compared with E9 (average thickness of fibers: 31.86±1.113 µm) and E6+72 h DMEM (average thickness of fibers: 29.86±4.214) groups. Neuron-specific TUJ1, CN and HU immunostainings show that the ENS is able to develop fully even in the presence of CXCR4 inhibition (Fig. 9C,F). To quantify the CN^{+} nerve fibers in the interplexus region, as well as the number of HU^{+} neurons, we measured the number of HU^{+} cells and CN^{+} interconnecting intrinsic fibers on cross-sections in each culture condition. When AMD3100 is added to the culture media, HU^{+} cells still colonize the entire hindgut (F). This was quantified by measuring the number of HU^{+} cells in E6+72 h DMEM (44.00±4.02) and AMD3100 (42.86±3.89) treated hindgut. In contrast, the number of CN^{+} nerve fibers was significantly reduced in AMD3100-treated intestines (7.43±2.59) compared with E6+72 h DMEM cultures (11.58±3.76).

Overexpression of Cxcl12 leads to increased extrinsic hindgut innervation

To determine whether CXCL12 could act as a chemoattractant factor for extrinsic nerve fibers *in ovo*, CXCL12-, AMD3100- or BSA-coated heparin beads were implanted into the wall of E5 pre-colonized hindgut and transplanted to E9 chicken CAM (Fig. 10A). Before bead implantation, the ceca and cloaca were removed to eliminate any intrinsic source of NCCs. After 8 days of incubation, guts were serially sectioned and analyzed for the presence of ENS and extrinsic nerve fibers. The graft develops normal smooth muscle layers and NoR in all conditions but has no enteric ganglion cells (Fig. 10B,C). Immunostaining of the graft demonstrates HU^{+}

Development (2023) 150, dev201289. doi:10.1242/dev.201289

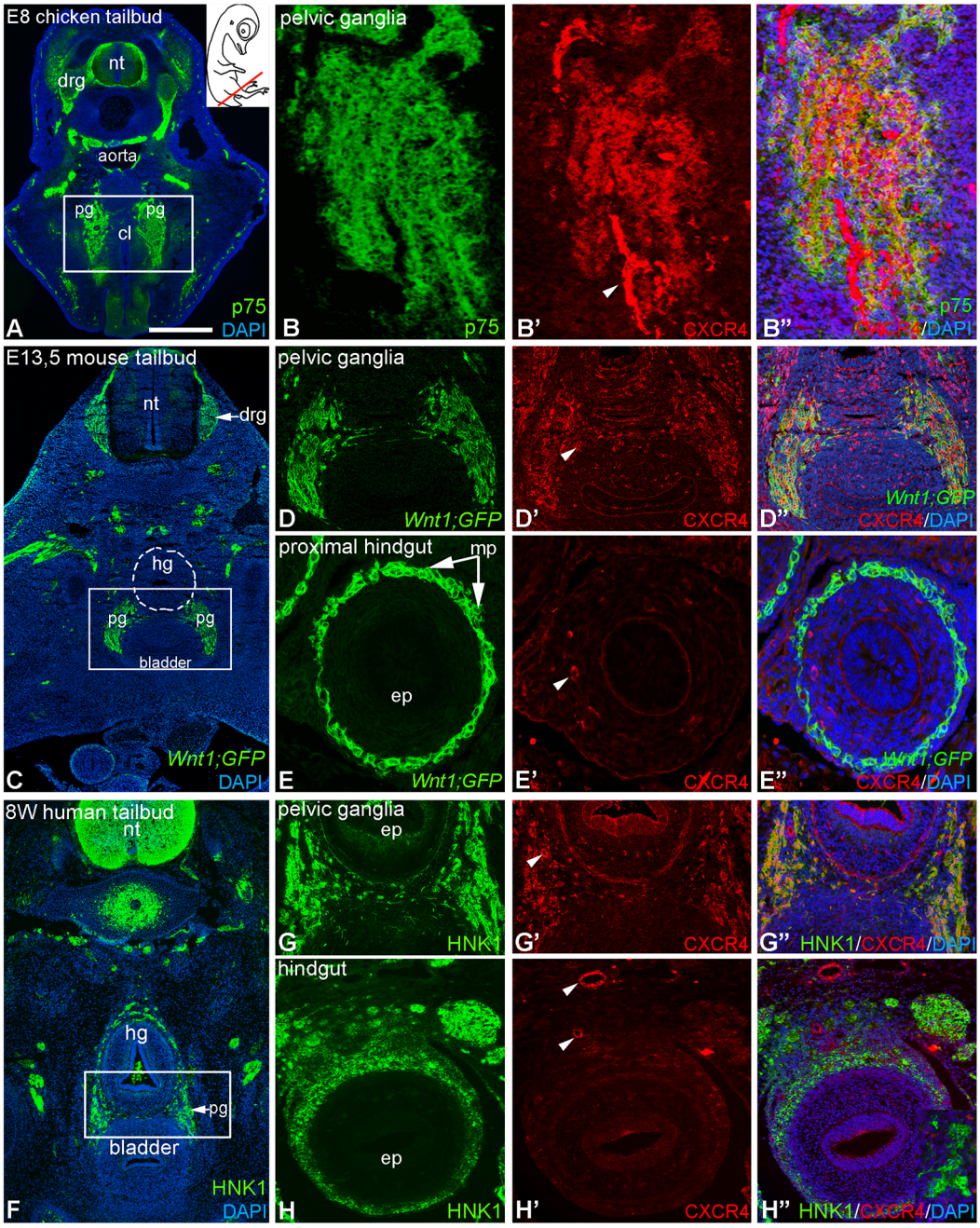

Fig. 5. Pelvic ganglia express CXCR4 in chick and mammalian embryos. (A-B″) Cross-sections of E8 chicken embryo tail bud show P75^{+} sacral neural crest-derived pelvic ganglia adjacent to the cloaca, with expression of CXCR4 present (A, outlined area is magnified in B-B″). (C) Similar to chicken, in mouse and human embryos the pelvic ganglia are located between the hindgut and bladder. (C-E″) E13.5 *Wnt1*:GFP mice. Cross-sections at the level of the pelvic ganglia show the co-expression of the CXCR4 receptor on sacral-derived NCCs. Area outlined in C is magnified in D-D″. (E-E″) In contrast, at the level of the proximal hindgut, the vagal-derived ENCCs do not express CXCR4. (F-H″) Eight-week-old human embryo. In a cross-section of the tail bud, the HNK1^{+} NCCs of the pelvic ganglia (G) express CXCR4 (G′). Area outlined in F is magnified in G-G″. (H-H″) Vagal crest-derived ENCCs in the hindgut are negative for CXCR4. Arrowheads indicate the CXCR4^{+} blood vessels. Scale bar: 450 µm (A); 110 µm (B-B″); 350 µm (C); 180 µm (D-D″); 90 µm (E-E″); 350 µm (F); 150 µm (G-G″); 120 µm (H-H″). nt, neural tube; drg, dorsal root ganglia; pg, pelvic ganglia; cl, cloaca; hg, hindgut; ep, midgut epithelium.

neurons (Fig. 10B) and BFABP^{+} glial cells (Fig. 10C) outside the wall of the gut, with no neuronal or glial cells present within the intestine. Despite the absence of ENS, TUJ1 immunoreactivity was present in the grafts (Fig. 10D), representing neuronal processes emanating from the NoR. Double immunofluorescence using antibodies to SOX10 and TUJ1 show the presence of SOX10^{+} cells associated with nerve fibers (Fig. 10D,E). In grafts transplanted with Cxcl12-coated beads placed near the developing NoR, the number of extrinsic nerve fibers of at least 30 µm in diameter are significantly increased (Fig. 10G) when compared with those exposed to BSA-coated (Fig. 10F) or AMD3100-coated beads (Fig. 10H). Local addition of AMD3100 to the hindgut did not interfere with gut wall development, but it did inhibit extrinsic nerve fiber formation, as shown by the absence or low number of TUJ1+ expressing neurons around the bead (Fig. 10H). The total number of nerve fibers was counted in CXCL12-, AMD3100- and BSA

Development (2023) 150, dev201289. doi:10.1242/dev.201289

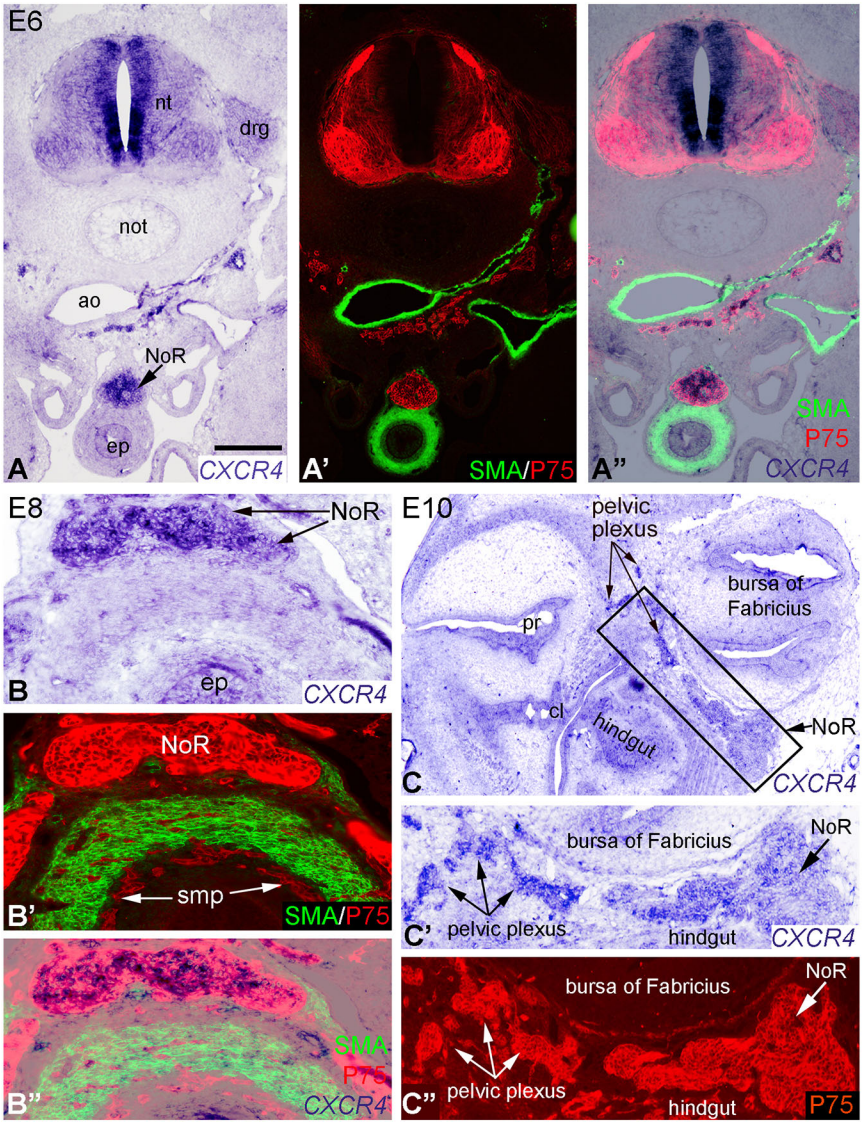

Fig. 6. *CXCR4* transcript is expressed in NoR and pelvic ganglia. *In situ* hybridization was performed to examine *CXCR4* expression in the developing hindgut and cloacal region. (A) At E6, *CXCR4* is highly expressed in the ventricular zone of the neural tube and NoR. (A′,A″) Triple staining of E6 hindgut by *CXCR4 in situ* hybridization with P75 (red) and α-smooth muscle actin (green) immunofluorescence shows that *CXCR4* overlaps with P75^{+} NoR but is not expressed by visceral smooth muscle. (B-B″). E8 hindgut cross-section stained for *CXCR4* (B), p75 (B′,B″) and α-smooth muscle actin (B′,B″) shows *CXCR4* transcript colocalized with P75^{+} NoR but not with vagal crest-derived ENS, as shown in the P75^{+}/*CXCR4*$^{-}$ submucosal plexus (smp). (C-C″) Sagittal section of E10 tailbud demonstrates *CXCR4* transcript in the distal part of the NoR and pelvic plexus. Area outlined in C is magnified in C′,C″, with P75 immunostaining shown. Scale bar: 350 µm (A-A″); 120 µm (B-B″); 370 µm (C); 180 µm (C′,C″). cl, cloaca; nt, neural tube; drg, dorsal root ganglia; not, notochord; ao, aorta; NoR, nerve of Remak; ep, hindgut epithelium; pr, proctodeum.

bead-treated hindguts, and the results are shown in Fig. 10I. After CXCL12-bead implantation, the thickness of TUJ1^{+} nerve fibers near the bead were also significantly increased. Nerve thickness around CXCL12 beads was 20.44 µm (±3.28) when compared with that around control beads (11.50±2.57 µm). TUJ1^{+} fiber density is significantly higher around CXCL12 beads (8.750±0.9857) than in case of control- (4.00±0.4082) or AMD3100-soaked beads (2.417 ±0.3128). We conclude that CXCL12 and/or CXCR4 signaling is required for NoR-derived extrinsic fiber formation in the hindgut.

DISCUSSION

In amniote embryos, hindgut innervation develops from multiple sources to form a complex neuroglial network. The majority of the ENS originates from vagal NCCs (first stream) that enter the foregut mesenchyme, turn caudally and migrate toward the cloaca to differentiate into enteric neurons and glia (Yntema and Hammond, 1954; Le Douarin and Teillet, 1973). The second stream arises from sacral NCCs that enter the dorsal mesentery and tail bud mesenchyme, migrate in a cranial direction, and contribute a small number of neurons and glia to the colorectal ENS (Nagy et al., 2007; Wang et al., 2011). NoR- and pelvic plexus-derived extrinsic nerves of sacral crest origin also innervate the hindgut (Burns and Le Douarin, 1998; Nagy et al., 2007, 2012). In mouse, postnatal neurogenesis occurs from Schwan cell precursors (SCPs) that invade the colon alongside the sacral crest-derived extrinsic nerves (third stream; Uesaka et al., 2015). Developmental abnormalities in any of these processes can result in congenital neurointestinal disorders, including Hirschsprung disease (HSCR), which is characterized by the absence of an ENS from the distal region of the gut. Interestingly, HSCR is often associated with the presence of hypertrophic extrinsic nerve fibers in the aganglionic segment (Kapur, 2016). However, despite extensive research on ENCC migration, proliferation and differentiation (Heanue et al., 2016; Nagy and Goldstein, 2017), the developmental mechanisms underlying extrinsic innervation of the colorectum are poorly understood (Uesaka et al., 2016). In the present study, results from migration assays using embryonic chicken hindgut and microbead implantation experiments combined with CAM grafts demonstrate that the Cxcl12 chemokine is a chemoattractant for CXCR4-expressing extrinsic nerves to innervate the hindgut, providing new information on this important and under-studied aspect of gut innervation.

The importance of CXCR4 and its ligand CXCL12 in NCC development is known (Shellard and Mayor, 2016). Previous findings

Development (2023) 150, dev201289. doi:10.1242/dev.201289

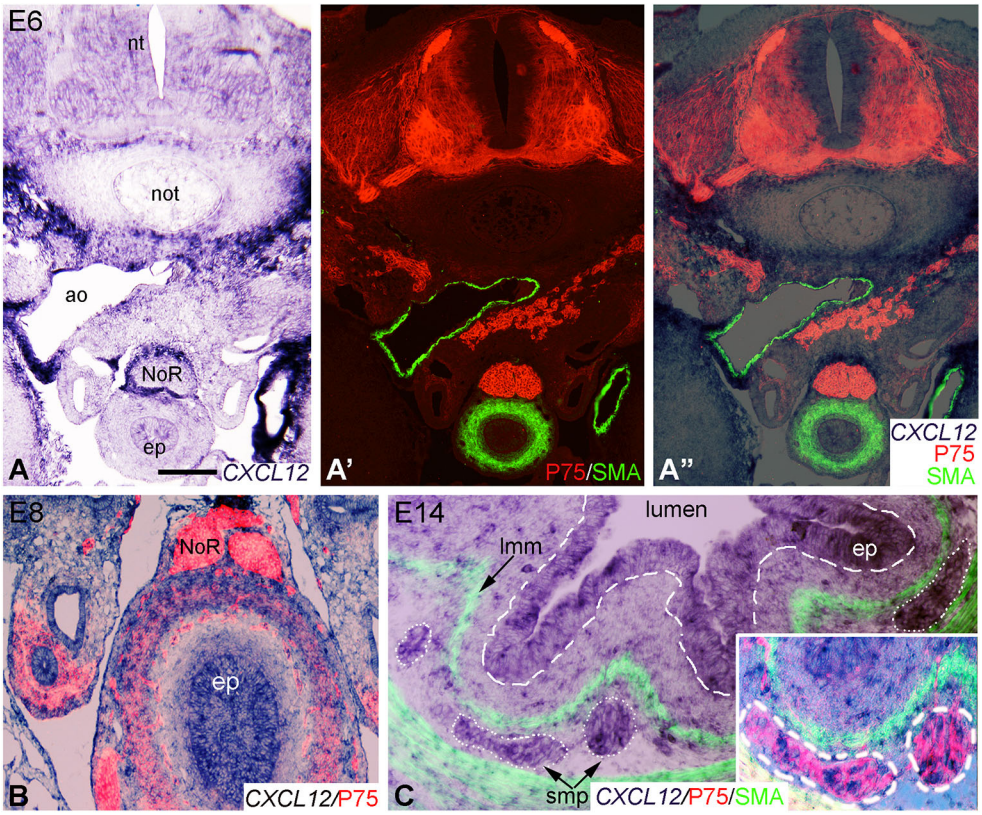

Fig. 7. Expression *of CXCL12* in developing chick hindgut. (A) Expression of *CXCL12* was examined in E6 (A-A″), E8 (B) and E14 (C) hindgut. (A) *In situ* hybridization shows *CXCL12* transcript in the mesenchyme around the NoR. Double staining of E6 and E8 hindgut by *CXCL12 in situ* hybridization and P75 immunofluorescence shows that *CXCL12* expression does not overlap with P75^{+} NoR. (A″) At E6, *CXCL12* is not co-expressed with α smooth muscle actin. (B) At E8, Cxcl12 transcript is seen in the epithelium and muscularis. (C) Double staining of E14 hindgut by *CXCL12 in situ* and P75 immunofluorescence (inset) shows that *CXCL12* is expressed by the gut epithelium and enteric ganglia. Scale bar: 250 µm (A-A″); 170 µm (B); 80 µm (C); 50 µm (C, inset). nt, neural tube; ao, aorta; not, notochord; NoR, nerve of Remak; ep, hindgut epithelium; lmm, lamina muscularis mucosae; smp, submucosal plexus.

demonstrate that, in early chicken embryos, CXCR4 is expressed by cardiac neural crest cells adjacent to CXCL12, producing the ectodermal and mesenchymal cells of the pharyngeal arches (Escot et al., 2013, 2016). Disruption of CXCR4 signaling in chicken and mouse embryos causes misrouting of cardiac NCCs and results in complex cardiac defects (Escot et al., 2016). CXCR4 signaling is also important in regulating migration of avian NCCs to the emerging sympathetic ganglia, but not dorsal root ganglia (Kasemeier-Kulesa et al., 2010). In contrast to chicken, defective positioning of dorsal root ganglia was observed in CXCR4 mutant mice (Belmadani et al., 2005). CXCR4 signaling plays an important role during zebrafish craniofacial development, whereas zebrafish trunk NCCs do not express CXCR4 (Olesnicky Killian et al., 2009). CXCL12 is also involved in regulating axonal growth of developing sensory neurons (Chalasani et al., 2003). Although many studies have uncovered various roles for CXCR4 and CXCL12 signaling in NCC trafficking and neuronal differentiation, little is known about the expression and function of these molecules in gut innervation.

We examined the expression of CXCR4 and CXCL12 during avian ENS development and found that CXCR4 was specifically expressed by vagal NCCs, as has been demonstrated in cardiac NCCs migrating toward the pharyngeal arches (Escot et al., 2013, 2016). Delaminating vagal NCCs from the neural tube expressed CXCR4 transiently, immediately before E3. Once the NCCs migrate below the level of the aorta, they gradually downregulate CXCR4 expression and show no further CXCR4 expression once they colonize the foregut mesenchyme. Interestingly, we find strong CXCR4 immunoreactivity (CXCR4^{high}) at the first three somite levels, where the cardiac subpopulation of vagal NCCs migrates in a dorsolateral direction, when compared with caudal to the 3rd somite, where CXCR4 immunoreactivity in vagal NCCs is less intense (CXCR4^{low}). We hypothesize that CXCR4^{high} and CXCR4^{low} vagal NCCs respond differently to CXCL12, and only the CXCR4^{high} NCCs from the cranial-most somites are able to respond to its chemoattractant effect, in agreement with our recent observations in B cell migration during development of the chicken bursa of Fabricius (Nagy et al., 2020). According to whole-mount staining by Escot et al. (2013), NCCs caudal to the 3rd somite show no expression of CXCR4. The discrepancy between the CXCR4 expression pattern in early chicken embryo could be explained by our more sensitive immunostaining of sectioned embryos. Our findings support the possibility that cardiac NCCs are segregated from the vagal NCC population based on the level of CXCR4 expression.

During avian ENS development, colonization of the colorectum by vagal-derived NCCs is completed by E8 and followed by the entry of sacral-derived NCCs around E10 (Burns and Le Douarin, 1998; Burns et al., 2000; Nagy et al., 2007). Before sacral NCCs enter the gut, NoR-derived fibers extend into the intestine as early as E7-E8 (HH31) (Teillet, 1978; Catala et al., 1995; Burns and Le Douarin, 1998). Using immunostaining and *in situ* hybridization approaches, we found that *CXCR4* is expressed in the NoR and pelvic plexus from E6 to E12. Distribution of *CXCL12* exhibits a complementary pattern in the developing hindgut, where *CXCL12* is expressed in the mesenchyme surrounding the *CXCR4*$^{+}$ nerve fibers. Once *CXCR4*$^{+}$ NoR-derived fibers penetrate the hindgut mesenchyme, *CXCL12* expression shifts to the outer muscularis layer and subsequently to the mucosa and enteric ganglia. This dynamic expression pattern of *CXCL12* may explain why NoR-derived highly fasciculated nerve fibers project first to the outer muscular wall of the colorectum and later innervate the ENS.

To investigate the contribution of NoR-derived extrinsic fibers to the hindgut ENS, we used CAM grafts. When ganglionic chick hindgut was recombined with GFP-labeled NoR and allowed to

Development (2023) 150, dev201289. doi:10.1242/dev.201289

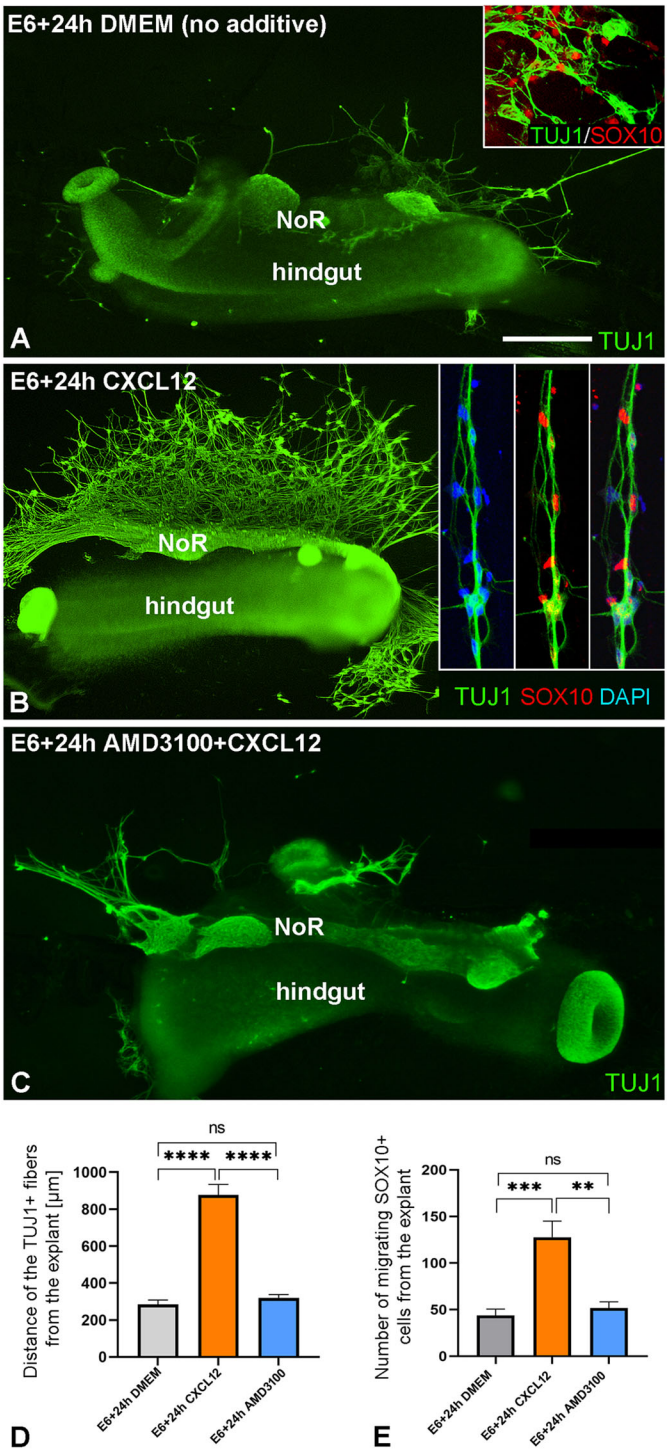

Fig. 8. CXCL12 promotes robust neurite outgrowth from explanted chicken NoR. (A-C) E6 gut was cultured on fibronectin-coated surface for 48 h in the absence (A) or presence (B) of CXCL12 or CXCL12+AMD3100 to assess nerve fiber outgrowth. (B) Addition of exogenous CXCL12 protein induced robust Tuj1$^+$ neurite extension from NoR. (C) The presence of AMD3100 inhibited this CXCL12-induced neuronal extension. Insets shows TUJ1$^+$ nerve fibers and SOX10$^+$ NCCs along the fibers. (D,E) Quantification of the length (µm) of TUJ1$^+$ fibers (D) and the number of SOX10$^+$ cells migrating from the explants (E). Compared with DMEM- and AMD3100-treated cultures, where a small number of SOX10$^+$ cells migrate a short distance away from the gut (A, inset), CXCL12-treated explants exhibit significantly more SOX10$^+$ cells. These migrate a greater distance from the hindgut and NoR, and are always associated with extending TUJ1$^+$ neurites. Kruskal–Wallis test with a post-hoc Dunn's test was used for D and E. ns, not significant; **P<0.01, ***P<0.001, ****P<0.0001. Data are mean±s.e.m. Scale bar: 400 µm (A-C); 50 µm (insets). NoR, nerve of Remak.

develop for 7 days, the grafts exhibited many nerve GFP$^+$ fibers projecting from the NoR into the outer hindgut mesenchyme, consistent with its role in extrinsic innervation of the colorectum (Aisa et al., 1998; Shepherd and Raper, 1999). We found no evidence that the NoR contributes neuronal cell bodies to the hindgut (as described by Le Douarin and Teilet, 1973; Catala et al., 1995; Nagy et al., 2007). CAM cultures of aneural hindgut with NoR demonstrated no NoR-derived ganglion cells in the transplanted gut, but extensive TUJ1$^+$ fibers projected from the NoR, and these were associated with a large number of SOX10$^+$ Schwann cells. This result supports the idea that CXCR4$^+$ nerve fibers from NoR penetrate the muscular wall and reach the enteric ganglia, and sacral NCC-derived Schwann cells migrate into the gut along these extrinsic sympathetic and parasympathetic nerve fibers (Teillet, 1978; Burns and Le Douarin, 1998; Nagy et al., 2007).

The projection of NoR axons to the hindgut in early development is restricted by the expression of collapsin 1 and/or semaphorin D (Shepherd and Raper, 1999). Downregulation of the chemorepellent collapsin 1 from the outer gut allows extrinsic nerve fibers from the NoR to innervate the muscularis layer. As hindgut expression of both CXCR4 and CXC12 occurs when NoR-derived fibers enter the hindgut, these molecules likely work with collapsin 1 to pattern extrinsic innervation of the colorectum. This model may be relevant to mammals, too, as CXCR4 is similarly expressed by the pelvic ganglia (Fig. 5) and semaphorin 3A is expressed by the distal hindgut mesenchyme (Anderson et al., 2007). Previous studies have demonstrated that CXCL12 exerts a modulatory effect on axon growth by reducing the repellent activities of multiple molecules, including slit 2, semaphorin 3A and semaphorin 3C (Chalasani et al., 2007). In addition, the location of CXCL12 expression in the developing chicken hindgut is similar to the distribution of the chemoattractive netrin molecule, which is expressed in the outer gut mesenchyme and mucosal epithelium (Jiang et al., 2003). Together, these findings suggest a possible interaction through which CXCL12-CXCR4 signaling, together with other chemorepellent and chemoattractive molecules, establishes the pattern for extrinsic axonal trajectories to the hindgut.

Cxcl12 or *Cxcr4* mutant mice die before birth and show defects in blood vessel formation, primordial germ cell migration, lymphopoiesis, gastrointestinal and nervous system development (Nagasawa et al., 1996, 1998; Tachibana et al., 1998; Zou et al., 1998). Indeed, it is known that several types of sensory neurons, sympathetic neurons and their precursors are affected in the presence of abnormal CXCR4 signaling (Belmadani et al., 2005; Kasemeier-Kulesa et al., 2010). In avian embryonic perturbation experiments using recombinant virus overexpressing dominant-negative (DN) CXCR4, ENS development was not affected, but *DN-Cxcr4* expressing cells failed to form the cardiac interventricular septum (Escot et al., 2013; Tang et al., 2021). Interestingly, in some of the *DN-Cxcr4*-infected chicken embryos, absence of NoR-derived extrinsic innervation to the hindgut was observed (Escot et al., 2013). The role of CXCL12-CXCR4 signaling in ENS development was also suggested by recent single cell RNAseq analysis, where upregulation of these molecules was reported in mouse (Memic et al., 2018) and avian embryos (Tang

Development (2023) 150, dev201289. doi:10.1242/dev.201289

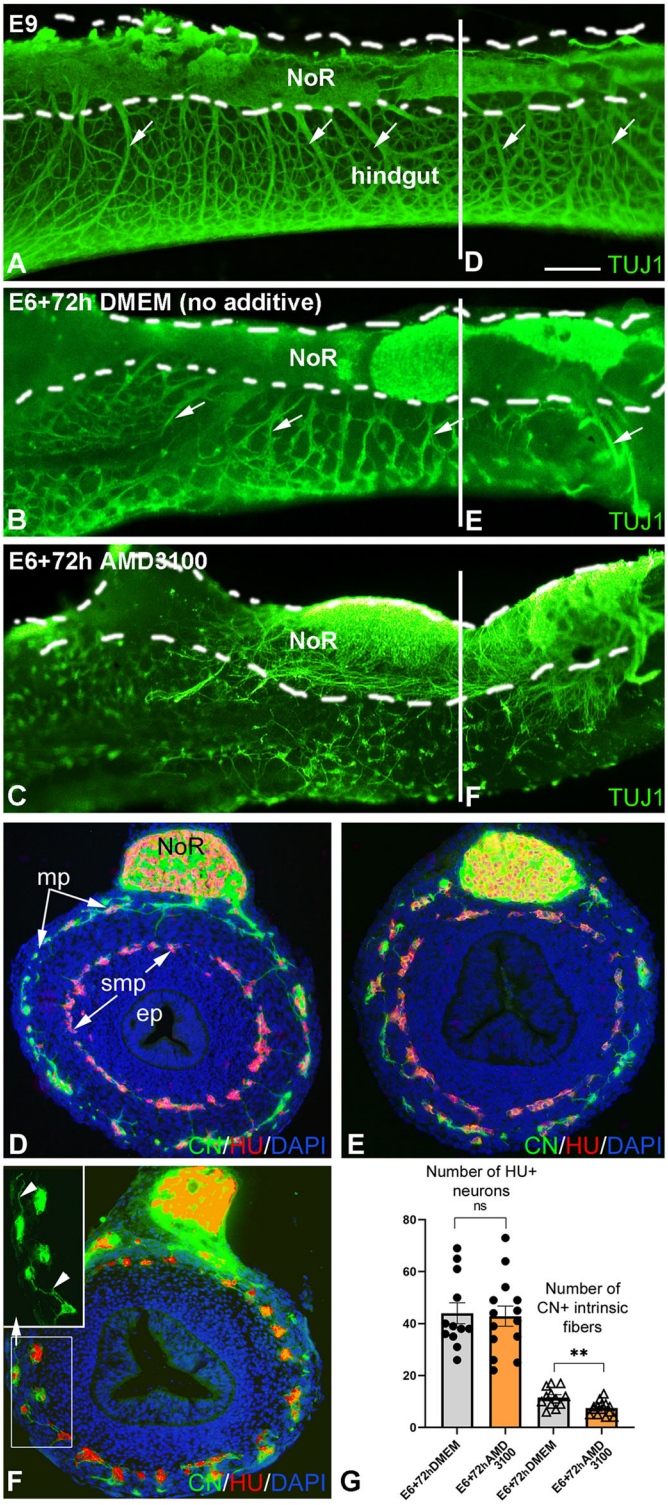

Fig. 9. Inhibition of CXCR4-CXCL12 signaling blocks extrinsic innervation of the hindgut. (A) Whole-mount TUJ1 immunofluorescence staining of E9 chick hindgut shows multiple neuronal fibers (arrows) extending from the NoR to the hindgut. (B,C) Explanted chick E6 hindgut was cultured in catenary culture for 72 h in DMEM (B) or with addition of the CXCR4 and CXCL12 signaling inhibitor AMD3100 (C) and immunolabeled using anti-TUJ1 antibodies. (C) NoR-derived extrinsic innervation of the hindgut was blocked by AMD3100 treatment. (D-F) Cross-sections through the hindgut, taken at the levels depicted in A-C, demonstrate the HU^+ neurons and CN^+ neuronal network in E9 hindgut (D), E6+72 h DMEM-treated (E) and E6+72 h AMD3100-treated (F) hindgut. (F) The inset from gut wall shows the CN^+ interconnecting nerve fibers between enteric plexuses. (G) Quantification of CN^+ fibers between myenteric and submucosal plexuses, and number of HU^+ enteric neurons. When AMD3100 is added to the culture media, HU^+ cells still colonize the entire hindgut (F). Although the number of HU^+ neurons was not affected, the number of CN^+ nerve fibers (F, inset arrowheads) was markedly reduced in AMD3100-treated hindgut (7.43±2.59) compared with E6+72 h DMEM cultures (11.58 ±3.76). NoR is outlined by a white dashed line in A-C. A Kruskal–Wallis test with a post-hoc Dunn's test was used for G. ns, not significant; $^{**}P<0.01$. Data are mean±s.e.m. Scale bars: 200 µm (A-C); 100 µm (D-F); 30 µm (F, inset). NoR, nerve of Remak; ep, hindgut epithelium; smp, submucosal plexus; mp, myenteric plexus.

et al., 2022 preprint preprint). Interestingly, in the latter study, *Cxcl12* transcripts were more abundant in the sacral NCC-derived population collected from E10 post-umbilical gut.

Treating intestinal explants with CXCL12 resulted in robust outgrowth of $TUJ1^+$ NoR-derived nerve fibers. The importance of CXCL12 signaling to hindgut development is further supported by the effect of AMD3100 on extrinsic fiber growth. AMD3100 is known to be a small molecule inhibitor of CXCR4 that is capable of disrupting the migration of cranial NCCs in avian embryos (Rezzoug et al., 2011). We observed a similar effect in the NoR, where AMD3100 treatment of explanted chicken hindgut blocked NoR-derived extrinsic fiber growth to the hindgut. We therefore conclude that CXCL12 expressed by the hindgut regulates the entry of extrinsic nerves into the colorectum through its receptor CXCR4.

Understanding the mechanisms underlying the development of extrinsic innervation to the hindgut has significant translational importance, particularly given its essential role in maintaining normal control of defecation. Congenital or acquired abnormalities in this extrinsic innervation, e.g. in spina bifida or traumatic injury, results in neurogenic bowel and has a major impact on quality of life. Defining the signaling pathways that control its development may therefore have important therapeutic implications in the future.

MATERIALS AND METHODS

Embryos

Fertilized White Leghorn chicken (*Gallus gallus domesticus*) eggs were obtained from commercial breeders (Prophyl-BIOVO, Hungary) and maintained at 37.5°C in a humidified incubator (HEKA 1+ egg incubator, Rietberg, Germany). Transgenic green fluorescent protein (GFP)-expressing chicken eggs were obtained from Prof. Helen Sang and Dr Adam Balic (The Roslin Institute, University of Edinburgh, UK) (McGrew et al., 2004). Embryos were staged according to the number of embryonic days (E) or to Hamburger and Hamilton (HH) tables (Hamburger and Hamilton, 1992). Gut development stages were referenced to the chick embryo gut staging table (Southwell, 2006) and the ENS formation timetable (Nagy et al., 2012). After developmental staging, the entire gut from E5-E10 chicken or segments of small and large intestines from older embryos were dissected out, fixed overnight in buffered 4% paraformaldehyde at 4°C and then processed for immunocytochemistry. Mice carrying the $Rosa26^{flox\text{-}mTRed\text{-}Stop\text{-}flox\text{-}mGFP}$ knock-in mutation (Muzumdar et al., 2007) were obtained from Dr Zoltan Jakus (Department of Physiology, Semmelweis University, Budapest, Hungary). Mice carrying the $Wnt1^{cre/+}$ knock-in allele (Danielian et al., 1998) were obtained from Dr Liam Ridge (UCL GOS Institute of Child Health, London, UK) and were maintained in heterozygous form. The two strains were crossed to obtain $Wnt1^{Cre/+}Rosa26^{mTmG/mTmG}$ (referred to as Wnt1-Cre/mTmG) mice in which all neural crest-derived cells are GFP labeled. All mice were on the C57BL/6 genetic background. Timed, pregnant mice sacrifice was carried out by exposure to rising levels of carbon dioxide followed by cervical dislocation, and the embryos were removed. The day of the vaginal plug was

Development (2023) 150, dev201289. doi:10.1242/dev.201289

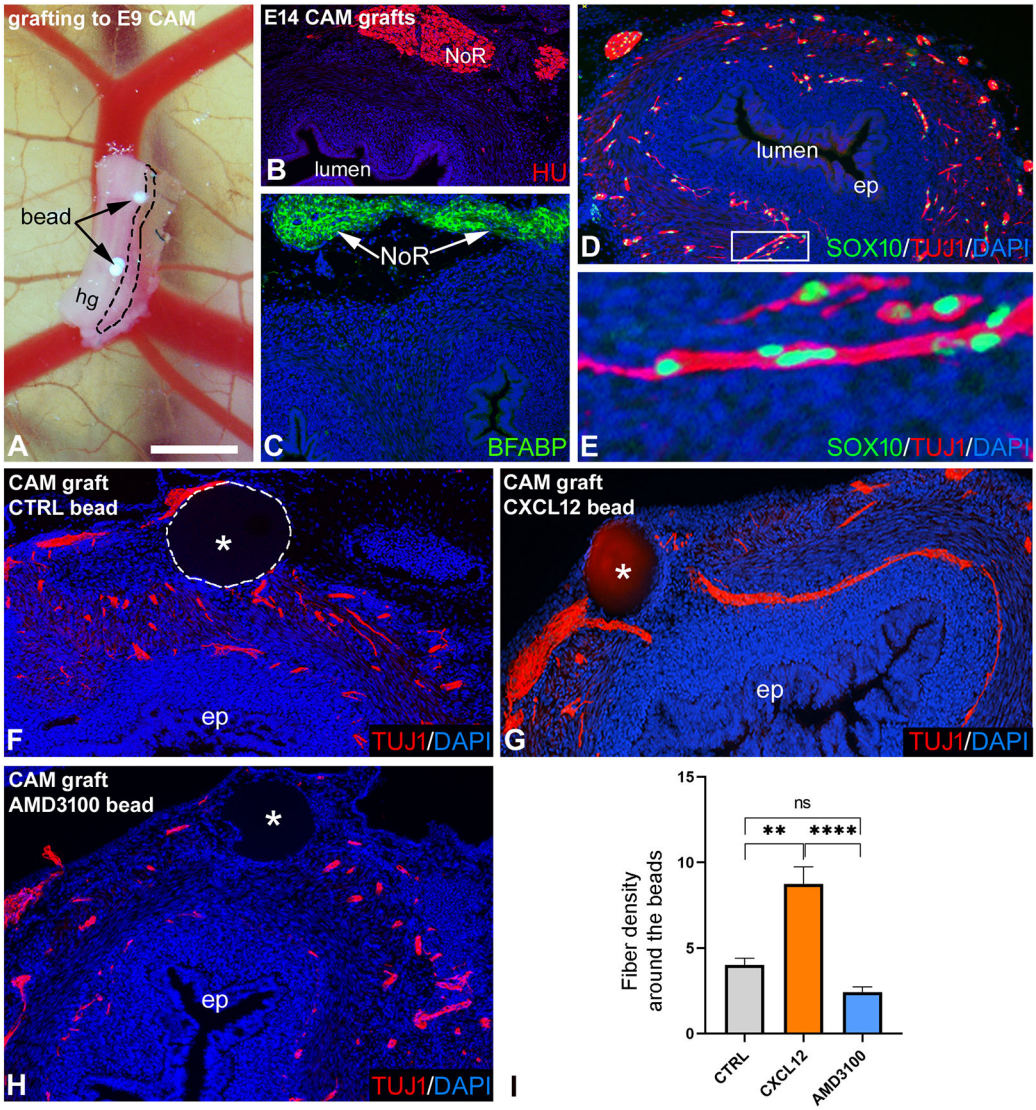

Fig. 10. Excess CXCL12 induces hypertrophic nerve formation in the hindgut. (A) Heparin beads soaked in 20 µg/ml CXCL12, 1 mM AMD3100 or 0.1% BSA were transplanted into the wall of E6 (pre-ganglionated) chick distal hindgut near the NoR and the hindgut was cultured on the chorioallantoic membrane (CAM) of an E9 host chick for an additional 8 days (dashed lines outline the NoR). (B,C) Immunostaining of the CAM graft demonstrates HU^+ neurons (B) and $BFABP^+$ glial cells (C) in the NoR, with no neuronal or glial cell bodies present within the gut wall. (D) TUJ1 immunostaining reveals many neuronal fibers extending into the graft, with $SOX10^+$ cells present along these extrinsic fibers. Area outlined in D is magnified in E. (F-H) In the presence of a CXCL12-soaked bead (G), the number of extrinsic fibers is significantly increased when compared with those exposed to AMD3100 (H) or BSA-treated beads (CTRL) (F). (I) Quantification of $TUJ1^+$ fiber density: the presence of a transplanted CXCL12 bead led to a significantly higher number of TUJ1 nerve fibers when compared with controls and AMD3100-treated guts. Kruskal–Wallis test with a post-hoc Dunn's test was used for I. ns, not significant; $^{**}P<0.01$; $^{****}P<0.0001$. Data are mean±s.e.m. Scale bar: 600 µm (A); 150 µm (B-D); 60 µm (E); 100µm (F-H). CAM, chorioallantoic membrane; hg, hindgut; NoR, nerve of Remak; ep, hindgut epithelium; hg, hindgut. Asterisks indicate the position of the bead.

considered 0.5 days post coitum. All animal experiments were approved by the Animal Experimentation Review Board of Semmelweis University. Remains of human embryos and fetuses (9–12 weeks after conception) were obtained after elective routine abortions with written consent given by the pregnant women. Histological work with the 4% PFA fixed (overnight at 4°C) human embryos has been ethically approved by the Regional and Institutional Committee of Science and Research Ethics, Semmelweis University (Research Ethics committee approval: 70/2012).

In vitro tissue recombination and chorioallantoic membrane transplants

To study the contribution of the NoR to the hindgut ENS, several different tissue recombination experiments in combination with chorioallantoic membrane (CAM) transplantation were performed. Briefly, to obtain aganglionic colon, the preganglionic hindgut grafts were prepared by isolating the postcecal intestine from E5 (HH 26) chick embryos. The cloacal region and the NoR were also removed using fine forceps and tungsten needles, and transplanted onto the CAM of E9 (HH 35) chick embryos as described previously (Nagy and Goldstein, 2006).

For NoR recombination experiments, NoR from E6 (HH 28) GFP-chick and non-GFP chick embryonic gut was separated from the midgut-hindgut segment. The NoR of the non-GFP chick embryo were replaced with NoR isolated from GFP-chick embryo. The proximal-distal orientation of the NoR was maintained in the recombination. To allow the tissues to adhere, NoR+intestine recombinations were embedded in a 3D collagen gel matrix (BD Biosciences; 354236) as described previously (Nagy et al., 2007). After overnight incubation, the recombinant chimeric hindgut was removed from the collagen gel and transplanted on the CAM of E8 chick then cultured for

Development (2023) 150, dev201289. doi:10.1242/dev.201289

7 days (n=5). At the end of culture period, the explants were excised, fixed overnight in 4% paraformaldehyde (PFA) at 4°C and embedded in gelatin for cryosectioning.

GFP-chick neural tube chimera

For extensive GFP labeling of the vagal neural crest, GFP-chick neural tube grafting were performed as previously described (Nagy et al., 2012; Delalande et al., 2021). Briefly, the neural tube and its associated neural crest, between somites 2 and 7, was microsurgically removed from normal chick embryos at the 10- to 11-somite stage of development (E1.5) and replaced with stage-matched equivalent tissue obtained from GFP-chick embryos. Following neural tube grafting, host eggs were returned to the incubator and further incubated up to an additional 7-9 days [number of chimeras analyzed with immunocytochemical methods (n)=5].

Intestinal organ culture assays

For the *in vitro* migration assay, hindgut was removed from E6 chick embryo and cultured on fibronectin-coated dishes in the presence of CXCL12 (100 ng/ml; R&D Systems, 6448-SD-025), GDNF (10 ng/ml; R&D Systems, 212-GD-010) or AMD3100 (200 µM, Sigma Aldrich, 155148-31-5) in DMEM culture media (Sigma Aldrich; D5429) for 24 h then processed for Tuj1 whole-mount immunofluorescence staining (n=5/culture condition).

For catenary culture (n=5 in each group), guts were removed from E5 (HH26) chick embryos, pinned down to silicone-coated tissue culture plates with insect pins, as described previously (Nagy et al., 2020), and allowed to float for 48 h in DMEM or culture media containing AMD3100 (200 µM). After 3 days of culture, guts were fixed overnight in 4% PFA at 4°C and processed for Tuj1 immunohistochemistry.

Microbead implantation

Heparin-Acrylic beads (70-150 µm diameter; Sigma Aldrich, H5263) were soaked in 20 µg/ml CXCL12 protein or 1 mM AMD3100 at 37°C for 1 h then beads were dried for 20 min at room temperature. Beads were inserted into the E6 hindgut mesenchyme, which was cultured on the CAM of E9 chicken embryo for an additional 8 days. 0.1% BSA in PBS-soaked beads served as a control. CAM grafts (n=5 in each group) were fixed overnight in 4% PFA at 4°C and embedded for cryosectioning. To quantify the thickness and number of nerve fibers, TUJ1 immunoreactive fibers within a 150 µm territory around the bead were counted. Data from six or seven independent hindgut+bead CAM grafts/experiment were collected for quantification.

Immunohistochemistry and image processing

Immunohistochemistry was performed as previously described (Nagy et al., 2012). For cryosections, tissue was fixed in 4% formaldehyde for 1 h, then incubated with 15% sucrose overnight at 4°C, infiltrated with 7.5% gelatin/15% sucrose in PBS for 1 h at 37°C, then rapidly frozen at −50°C in methylbutane (Sigma-Aldrich, 78-78-4). Cryosections (12 µm) were stained using the following primary antibodies: anti-human p75 (1:200, Promega, G3231), which recognizes the cytoplasmic domain of the p75 neurotrophin receptor on the surface of the mouse neural crest-derived cells; anti-chicken p75 (kind gift from Dr Louis Reichardt; Weskamp and Reichardt, 1991); anti-SOX10 (1:30, clone A-2, Santa Cruz Biotechnology, sc-365692); anti-chicken CXCR4 (1:100; clone 9D9); anti-HuC/D (clone 16A11, 1:50, Thermo Fisher Scientific, A-21271), which recognizes a neuron-specific RNA-binding protein; anti-Tuj1 (clone B1195, 1:400, Covance, MMS-435P), a neuron-specific class III beta-tubulin; BFABP (brain fatty acid binding protein, 1:50, Kurtz et al., 1994); anti-collagen type 18 (clone 6C4, 1:5, Developmental Studies Hybridoma Bank, AB 528177); anti-alpha smooth muscle actin (clone 1A4, 1:400,Thermo Fisher, 14-9760-82); anti-GFP (green florescent protein, 1:200, Rockland, 600-101-215 M); anti-CN, a chicken-specific neurite marker (Kuratani and Tanaka, 1990); anti-nNOS (clone 3G6B10, 1:200, Thermo Fisher Scientific); and anti-neurofilament (clone: 2F11, 1:50, NeoMarkers). Primary antibodies were applied for 45 min, followed by Alexa-conjugated fluorescent secondary antibodies: Alexa Fluor 488 goat anti-mouse IgG (1:200, A32723), Alexa Fluor 594 goat anti-mouse IgG (1:200, A32742), Alexa Fluor 488 goat anti-mouse IgG1 (1:200, A21121), Alexa Fluor 594 goat anti-mouse IgG1 (1:200, A21125), Alexa Fluor 594 goat anti-mouse IgG2a (1:200, A21135), Alexa Fluor 594 goat anti-mouse IgM (1:200, A21044), Alexa Fluor 488 donkey anti-goat IgG (1:200, A11055), Alexa Fluor 488 goat anti-rabbit IgG (1:200, A32731) and Alexa Fluor 546 goat anti-rabbit IgG (1:200, A11035), all from Thermo Fisher Scientific. Cell nuclei were stained with 40,6-diamidino-2-phenylindole (DAPI; Vector Labs, Burlingame, California). The sections were covered by aqueous Poly-Mount (Polyscience, 18606).

For whole-mount immunofluorescent staining, hindguts were fixed overnight in 4% PFA at 4°C, permeabilized with 1% normal goat serum and 0.1% Triton X-100 (Sigma Aldrich, 9036-19-5) in PBS overnight at 4°C. Specimens were labeled overnight using anti-Tuj1 (1:400) at 4°C. After washing in PBS, fluorescent secondary antibody (Alexa Fluor 488 goat anti-mouse, 1:100, A32723) was applied for 1 h.

Section images were recorded using a Nikon Eclipse E800 fluorescence microscope and Zeiss LSM 710 confocal microscope, whole-mount images were recorded using a Nikon SMZ25 (with Prior L200/E unit) fluorescence stereomicroscope. Image processing, including tiling and merging of pseudocolored immunofluorescent images, used CellSens, ZEISS ZEN Imaging, Nis-Elements (v 5.02) Imaging proprietary software and ImageJ (http://rsb.info.nih.gov/ij/).

In situ hybridization

In situ hybridization was performed for chick *Cxcr4* and *Cxcl12* genes on paraffin wax-embedded sections using digoxigenin-labeled riboprobes (plasmids were kindly provided by Dr Beate Brand-Saberi, Ruhr-Universität Bochum, Germany; Rehimi et al., 2008, 2010). Riboprobe synthesis and *in situ* hybridization were performed according to standard protocols (Acloque et al., 2008).

Statistical analysis

Statistical analysis was performed by Kruskal–Wallis test with a post-hoc Dunn's test (Figs 4, 8 and 9), one-way ANOVA with Tukey's multiple comparisons test (Fig. 9) and a Mann–Whitney U test (CXCR4 immunofluorescence intensity, Fig. 1B) (Graphpad Prism v9.4.1). The P-value was adjusted with Holm correction. P<0.05 was considered significant (ns, not significant; *P<0.05, **P<0.01, ***P<0.001, ****P<0.0001). Error bars represent s.e.m.

Competing interests

The authors declare no competing or financial interests.

Author contributions

Conceptualization: V.H., A.M.G., N.N.; Methodology: V.H., E.S., A.S., T.K., N.P.-F., N.N.; Software: V.H., A.S.; Validation: V.H., E.S., A.S.; Formal analysis: V.H., E.S., A.S., R.H.; Investigation: V.H., E.S., N.N.; Resources: R.H., N.N.; Data curation: V.H., A.S., N.P.-F.; Writing - original draft: V.H., N.N.; Writing - review & editing: A.M.G., N.N.; Visualization: V.H., E.S., T.K., N.P.-F., N.N.; Supervision: N.N.; Project administration: N.N.; Funding acquisition: N.N.

Funding

This work was supported by the National Institutes of Health (R01DK119210 and R21HD106036 to A.M.G.); by the Research Excellence Programme of the Innovációs és Technológiai Minisztérium (Hungary), within the framework of the TKP2021-EGA-25 thematic programme of Semmelweis University (to N.N.); and by a Hungarian Science Foundation NKFI grant [138664 to N.N.]. Deposited in PMC for release after 12 months.

Data availability

All relevant data can be found within the article and its supplementary information.

Peer review history

The peer review history is available online at https://journals.biologists.com/dev/lookup/doi/10.1242/dev.201289.reviewer-comments.pdf

References

Acloque, H., Wilkinson, D. G. and Nieto, M. A. (2008). *In situ* hybridization analysis of chick embryos in whole-mount and tissue sections. *Methods Cell Biol.* **87**, 169-185. doi:10.1016/S0091-679X(08)00209-4

Aisa, J., Lahoz, M., Serrano, P. J., Castiella, T., Junquera, C., Azanza, M. J. and Vera-Gil, A. (1998). Histochemical, immunohistochemical, and electron

microscopy study of the caudal portion of the chicken intestinal nerve of Remak. *Neurochem. Res.* **23**, 845-853. doi:10.1023/A:1022454827533

Anderson, R. B., Bergner, A. J., Taniguchi, M., Fujisawa, H., Forrai, A., Robb, L. and Young, H. M. (2007). Effects of different regions of the developing gut on the migration of enteric neural crest-derived cells: a role for Sema3A, but not Sema3F. *Dev. Biol.* **305**, 287-299. doi:10.1016/j.ydbio.2007.02.020

Belmadani, A., Tran, P. B., Ren, D., Assimacopoulos, S., Grove, E. A. and Miller, R. J. (2005). The chemokine stromal cell-derived factor-1 regulates the migration of sensory neuron progenitors. *J. Neurosci.* **25**, 3995-4003. doi:10.1523/JNEUROSCI.4631-04.2005

Bhardwaj, D., Náger, M., Camats, J., David, M., Benguria, A., Dopazo, A., Cantí, C. and Herreros, J. (2013). Chemokines induce axon outgrowth downstream of Hepatocyte Growth Factor and TCF/β-catenin signaling. *Front. Cell Neurosci.* **7**, 52. doi:10.3389/fncel.2013.00052

Burns, A. J. and Le Douarin, N. M. (1998). The sacral neural crest contributes neurons and glia to the post-umbilical gut: spatiotemporal analysis of the development of the enteric nervous system. *Development* **125**, 4335-4347. doi:10.1242/dev.125.21.4335

Burns, A. J., Champeval, D. and Le Douarin, N. M. (2000). Sacral neural crest cells colonise aganglionic hindgut *in vivo* but fail to compensate for lack of enteric ganglia. *Dev. Biol.* **219**, 30-43. doi:10.1006/dbio.1999.9592

Catala, M., Teillet, M. A. and Le Douarin, N. M. (1995). Organization and development of the tail bud analyzed with the quail-chick chimaera system. *Mech. Dev.* **51**, 51-65. doi:10.1016/0925-4773(95)00350-A

Chalasani, S. H., Sabelko, K. A., Sunshine, M. J., Littman, D. R. and Raper, J. A. (2003). A chemokine, SDF-1, reduces the effectiveness of multiple axonal repellents and is required for normal axon pathfinding. *J. Neurosci.* **23**, 1360-1371. doi:10.1523/JNEUROSCI.23-04-01360.2003

Chalasani, S. H., Sabol, A., Xu, H., Gyda, M. A., Rasband, K., Granato, M., Chien, C. B. and Raper, J. A. (2007). Stromal cell-derived factor-1 antagonizes slit/robo signaling *in vivo*. *J. Neurosci.* **27**, 973-980. doi:10.1523/JNEUROSCI.4132-06.2007

Chen, T., Bai, H., Shao, Y., Arzigian, M., Janzen, V., Attar, E., Xie, Y., Scadden, D. T. and Wang, Z. Z. (2007). Stromal cell-derived factor-1/CXCR4 signaling modifies the capillary-like organization of human embryonic stem cell-derived endothelium *in vitro*. *Stem Cells* **25**, 392-401. doi:10.1634/stemcells.2006-0145

Cheng, X., Wang, H., Zhang, X., Zhao, S., Zhou, Z., Mu, X., Zhao, C. and Teng, W. (2017). The role of SDF-1/CXCR4/CXCR7 in neuronal regeneration after cerebral ischemia. *Front. Neurosci.* **11**, 590. doi:10.3389/fnins.2017.00590

Danielian, P. S., Muccino, D., Rowitch, D. H., Michael, S. K. and Mcmahon, A. P. (1998). Modification of gene activity in mouse embryos *in utero* by a tamoxifen-inducible form of Cre recombinase. *Curr. Biol.* **8**, 1323-1326. doi:10.1016/S0960-9822(07)00562-3

Delalande, J. M., Nagy, N., Mccann, C. J., Natarajan, D., Cooper, J. E., Carreno, G., Dora, D., Campbell, A., Laurent, N., Kemos, P. et al. (2021). TALPID3/KIAA0586 regulates multiple aspects of neuromuscular patterning during gastrointestinal development in animal models and Human. *Front. Mol. Neurosci.* **14**, 757646. doi:10.3389/fnmol.2021.757646

Doitsidou, M., Reichman-Fried, M., Stebler, J., Köprunner, M., Dörries, J., Meyer, D., Esguerra, C. V., Leung, T. and Raz, E. (2002). Guidance of primordial germ cell migration by the chemokine SDF-1. *Cell* **111**, 647-659. doi:10.1016/S0092-8674(02)01135-2

Escot, S., Blavet, C., Härtle, S., Duband, J. L. and Fournier-Thibault, C. (2013). Misregulation of SDF1-CXCR4 signaling impairs early cardiac neural crest cell migration leading to conotruncal defects. *Circ. Res.* **113**, 505-516. doi:10.1161/CIRCRESAHA.113.301333

Escot, S., Blavet, C., Faure, E., Zaffran, S., Duband, J. L. and Fournier-Thibault, C. (2016). Disruption of CXCR4 signaling in pharyngeal neural crest cells causes DiGeorge syndrome-like malformations. *Development* **143**, 582-588. doi:10.1242/dev.126573

Espinosa-Medina, I., Jevans, B., Boismoreau, F., Chettouh, Z., Enomoto, H., Müller, T., Birchmeier, C., Burns, A. J. and Brunet, J. F. (2017). Dual origin of enteric neurons in vagal Schwann cell precursors and the sympathetic neural crest. *Proc. Natl. Acad. Sci. USA* **114**, 11980-11985. doi:10.1073/pnas.1710308114

Goldstein, A. M., Thapar, N., Karunaratne, T. B. and De Giorgio, R. (2016). Clinical aspects of neurointestinal disease: pathophysiology, diagnosis, and treatment. *Dev. Biol.* **417**, 217-228. doi:10.1016/j.ydbio.2016.03.032

Hamburger, V. and Hamilton, H. L. (1992). A series of normal stages in the development of the chick embryo. 1951. *Dev. Dyn.* **195**, 231-272. doi:10.1002/aja.1001950404

Heanue, T. A., Shepherd, I. T. and Burns, A. J. (2016). Enteric nervous system development in avian and zebrafish models. *Dev. Biol.* **417**, 129-138. doi:10.1016/j.ydbio.2016.05.017

Hearn, C. and Newgreen, D. (2000). Lumbo-sacral neural crest contributes to the avian enteric nervous system independently of vagal neural crest. *Dev. Dyn.* **218**, 525-530. doi:10.1002/1097-0177(200007)218:3<525::AID-DVDY1003>3.0.CO;2-7

Hilla, A. M., Baehr, A., Leibinger, M., Andreadaki, A. and Fischer, D. (2021). CXCR4/CXCL12-mediated entrapment of axons at the injury site compromises optic nerve regeneration. *Proc. Natl. Acad. Sci. USA*. **118**, e2016409118. doi:10.1073/pnas.2016409118

Jiang, Y., Liu, M. T. and Gershon, M. D. (2003). Netrins and DCC in the guidance of migrating neural crest-derived cells in the developing bowel and pancreas. *Dev. Biol.* **258**, 364-384. doi:10.1016/S0012-1606(03)00136-2

Kang, Y. N., Fung, C. and Vanden Berghe, P. (2021). Gut innervation and enteric nervous system development: a spatial, temporal and molecular tour de force. *Development* **148**, dev182543. doi:10.1242/dev.182543

Kapur, R. P. (2000). Colonization of the murine hindgut by sacral crest-derived neural precursors: experimental support for an evolutionarily conserved model. *Dev. Biol.* **227**, 146-155. doi:10.1006/dbio.2000.9886

Kapur, R. P. (2016). Histology of the transition zone in hirschsprung disease. *Am. J. Surg. Pathol.* **40**, 1637-1646. doi:10.1097/PAS.0000000000000711

Kasemeier-Kulesa, J. C., Mclennan, R., Romine, M. H., Kulesa, P. M. and Lefcort, F. (2010). CXCR4 controls ventral migration of sympathetic precursor cells. *J. Neurosci.* **30**, 13078-13088. doi:10.1523/JNEUROSCI.0892-10.2010

Kirchgessner, A. L. and Gershon, M. D. (1990). Innervation of the pancreas by neurons in the gut. *J. Neurosci.* **10**, 1626-1642. doi:10.1523/JNEUROSCI.10-05-01626.1990

Kuratani, S. and Tanaka, S. (1990). Peripheral development of the avian vagus nerve with special reference to the morphological innervation of heart and lung. *Anat. Embryol.* **182**, 435-445. doi:10.1007/BF00178908

Kurtz, A., Zimmer, A., Schnütgen, F., Brüning, G., Spener, F. and Müller, T. (1994). The expression pattern of a novel gene encoding brain-fatty acid binding protein correlates with neuronal and glial cell development. *Development* **120**, 2637-2649. doi:10.1242/dev.120.9.2637

Le Douarin, N. M. and Teillet, M. A. (1973). The migration of neural crest cells to the wall of the digestive tract in avian embryo. *J. Embryol. Exp. Morphol.* **30**, 31-48.

Lieberam, I., Agalliu, D., Nagasawa, T., Ericson, J. and Jessell, T. M. (2005). A Cxcl12-CXCR4 chemokine signaling pathway defines the initial trajectory of mammalian motor axons. *Neuron* **47**, 667-679. doi:10.1016/j.neuron.2005.08.011

Margarido, A. S., Le Guen, L., Falco, A., Faure, S., Chauvet, N. and De Santa Barbara, P. (2020). PROX1 is a specific and dynamic marker of sacral neural crest cells in the chicken intestine. *J. Comp. Neurol.* **528**, 879-889. doi:10.1002/cne.24801

Mcgrath, K. E., Koniski, A. D., Maltby, K. M., Mcgann, J. K. and Palis, J. (1999). Embryonic expression and function of the chemokine SDF-1 and its receptor, CXCR4. *Dev. Biol.* **213**, 442-456. doi:10.1006/dbio.1999.9405

Mcgrew, M. J., Sherman, A., Ellard, F. M., Lillico, S. G., Gilhooley, H. J., Kingsman, A. J., Mitrophanous, K. A. and Sang, H. (2004). Efficient production of germline transgenic chickens using lentiviral vectors. *EMBO Rep.* **5**, 728-733. doi:10.1038/sj.embor.7400171

Memic, F., Knoflach, V., Morarac,, K., Sadler, R., Laranjeira, C., Hjerling-Leffler, J., Sundström, E., Pachnis, V. and Marklund, U. (2018). Transcription and signaling regulators in developing neuronal subtypes of mouse and human enteric nervous system. *Gastroenterology* **154**, 624-636. doi:10.1053/j.gastro.2017.10.005

Muzumdar, M. D., Tasic, B., Miyamichi, K., Li, L. and Luo, L. (2007). A global double-fluorescent Cre reporter mouse. *Genesis* **45**, 593-605. doi:10.1002/dvg.20335

Nagasawa, T., Hirota, S., Tachibana, K., Takakura, N., Nishikawa, S., Kitamura, Y., Yoshida, N., Kikutani, H. and Kishimoto, T. (1996). Defects of B-cell lymphopoiesis and bone-marrow myelopoiesis in mice lacking the CXC chemokine PBSF/SDF-1. *Nature* **382**, 635-638. doi:10.1038/382635a0

Nagasawa, T., Tachibana, K. and Kishimoto, T. (1998). A novel CXC chemokine PBSF/SDF-1 and its receptor CXCR4: their functions in development, hematopoiesis and HIV infection. *Semin. Immunol.* **10**, 179-185. doi:10.1006/smim.1998.0128

Nagy, N. and Goldstein, A. M. (2006). Endothelin-3 regulates neural crest cell proliferation and differentiation in the hindgut enteric nervous system. *Dev. Biol.* **293**, 203-217. doi:10.1016/j.ydbio.2006.01.032

Nagy, N. and Goldstein, A. M. (2017). Enteric nervous system development: a crest cell's journey from neural tube to colon. *Semin. Cell Dev. Biol.* **66**, 94-106. doi:10.1016/j.semcdb.2017.01.006

Nagy, N., Brewer, K. C., Mwizerwa, O. and Goldstein, A. M. (2007). Pelvic plexus contributes ganglion cells to the hindgut enteric nervous system. *Dev. Dyn.* **236**, 73-83. doi:10.1002/dvdy.20933

Nagy, N., Burns, A. J. and Goldstein, A. M. (2012). Immunophenotypic characterization of enteric neural crest cells in the developing avian colorectum. *Dev. Dyn.* **241**, 842-851. doi:10.1002/dvdy.23767

Nagy, N., Guyer, R. A., Hotta, R., Zhang, D., Newgreen, D. F., Halasy, V., Kovacs, T. and Goldstein, A. M. (2020). RET overactivation leads to concurrent Hirschsprung disease and intestinal ganglioneuromas. *Development***147**, dev190900. doi:10.1242/dev.190900

Nagy, N., Kovacs, T., Stavely, R., Halasy, V., Soos, A., Szocs, E., Hotta, R., Graham, H. and Goldstein, A. M. (2021). Avian ceca are indispensable for hindgut enteric nervous system development. *Development* **148**, dev199825. doi:10.1242/dev.199825

Niu, X., Liu, L., Wang, T., Chuan, X., Yu, Q., Du, M., Gu, Y. and Wang, L. (2020). Mapping of extrinsic innervation of the gastrointestinal tract in the mouse embryo. *J. Neurosci.* **40**, 6691-6708. doi:10.1523/JNEUROSCI.0309-20.2020

Nolf, P. (1934). Les nerfs extrinsiques de l'intestin chez l'Oiseau. Le neff de Remak. *Arch. int. Physiol.* **39**, 227-256.

Olesnicky Killian, E. C., Birkholz, D. A. and Artinger, K. B. (2009). A role for chemokine signaling in neural crest cell migration and craniofacial development. *Dev. Biol.* **333**, 161-172. doi:10.1016/j.ydbio.2009.06.031

Pomeranz, H. D., Rothman, T. P. and Gershon, M. D. (1991). Colonization of the post-umbilical bowel by cells derived from the sacral neural crest: direct tracing of cell migration using an intercalating probe and a replication-deficient retrovirus. *Development* **111**, 647-655. doi:10.1242/dev.111.3.647

Rao, M. and Gershon, M. D. (2016). The bowel and beyond: the enteric nervous system in neurological disorders. *Nat. Rev. Gastroenterol. Hepatol.* **13**, 517-528. doi:10.1038/nrgastro.2016.107

Rehimi, R., Khalida, N., Yusuf, F., Dai, F., Morosan-Puopolo, G. and Brand-Saberi, B. (2008). Stromal-derived factor-1 (SDF-1) expression during early chick development. *Int. J. Dev. Biol.* **52**, 87-92. doi:10.1387/ijdb.072374rr

Rehimi, R., Khalida, N., Yusuf, F., Morosan-Puopolo, G. and Brand-Saberi, B. (2010). A novel role of CXCR4 and SDF-1 during migration of cloacal muscle precursors. *Dev. Dyn.* **239**, 1622-1631. doi:10.1002/dvdy.22288

Rezzoug, F., Seelan, R. S., Bhattacherjee, V., Greene, R. M. and Pisano, M. M. (2011). Chemokine-mediated migration of mesencephalic neural crest cells. *Cytokine* **56**, 760-768. doi:10.1016/j.cyto.2011.09.014

Schneider, S., Wright, C. M. and Heuckeroth, R. O. (2019). Unexpected roles for the second brain: enteric nervous system as master regulator of bowel function. *Annu. Rev. Physiol.* **81**, 235-259. doi:10.1146/annurev-physiol-021317-121515

Serbedzija, G. N., Burgan, S., Fraser, S. E. and Bronner-Fraser, M. (1991). Vital dye labeling demonstrates a sacral neural crest contribution to the enteric nervous system of chick and mouse embryos. *Development* **111**, 857-866. doi:10.1242/dev.111.4.857

Shellard, A. and Mayor, R. (2016). Chemotaxis during neural crest migration. *Semin. Cell. Dev. Biol.* **55**, 111-118. doi:10.1016/j.semcdb.2016.01.031

Shepherd, I. T. and Raper, J. A. (1999). Collapsin-1/semaphorin D is a repellent for chick ganglion of Remak axons. *Dev. Biol.* **212**, 42-53. doi:10.1006/dbio.1999.9294

Shihan, M. H., Novo, S. G., Le Marchand, S. J., Wang, Y. and Duncan, M. K. (2021). A simple method for quantitating confocal fluorescent images. *Biochem. Biophys. Rep.* **25**, 100916. doi:10.1016/j.bbrep.2021.100916

Southwell, B. R. (2006). Staging of intestinal development in the chick embryo. *Anat. Rec. A. Discov. Mol. Cell. Evol. Biol.* **288A**, 909-920. doi:10.1002/ar.a.20349

Suzuki, M., Ohmori, Y. and Watanabe, T. (1996). Projections of neurons in the intestinal nerve of Remak to the chicken intestine. *J. Auton. Nerv. Syst.* **61**, 79-86. doi:10.1016/0165-1838(96)00061-6

Tachibana, K., Hirota, S., Iizasa, H., Yoshida, H., Kawabata, K., Kataoka, Y., Kitamura, Y., Matsushima, K., Yoshida, N., Nishikawa, S. et al. (1998). The chemokine receptor CXCR4 is essential for vascularization of the gastrointestinal tract. *Nature* **393**, 591-594. doi:10.1038/31261

Tanaka, D. H., Mikami, S., Nagasawa, T., Miyazaki, J., Nakajima, K. and Murakami, F. (2010). CXCR4 is required for proper regional and laminar distribution of cortical somatostatin-, calretinin-, and neuropeptide Y-expressing GABAergic interneurons. *Cereb. Cortex* **20**, 2810-2817. doi:10.1093/cercor/bhq027

Tang, W., Li, Y., Li, A. and Bronner, M. E. (2021). Clonal analysis and dynamic imaging identify multipotency of individual *Gallus gallus* caudal hindbrain neural crest cells toward cardiac and enteric fates. *Nat. Commun.* **12**, 1894. doi:10.1038/s41467-021-22146-8

Tang, W., Jacobs-Li, J., Li, C. and Bronner, M. E. (2022). Single-cell profiling coupled with lineage analysis reveals distinct sacral neural crest contributions to the developing enteric nervous system. *bioRxiv*. doi:10.1101/2022.05.09.491197

Teillet, M. A. (1978). Evolution of the lumbo-sacral neural crest in the avian embryo: origin and differentiation of the ganglionated nerve of Remak studied in interspecific quail-chick chimaerae. *Wilhelm Roux's Arch. Dev. Biol.* **184**, 251-268. doi:10.1007/BF00848257

Uesaka, T., Nagashimada, M. and Enomoto, H. (2015). Neuronal differentiation in Schwann cell lineage underlies postnatal neurogenesis in the enteric nervous system. *J. Neurosci.* **35**, 9879-9888. doi:10.1523/JNEUROSCI.1239-15.2015

Uesaka, T., Young, H. M., Pachnis, V. and Enomoto, H. (2016). Development of the intrinsic and extrinsic innervation of the gut. *Dev. Biol.* **417**, 158-167. doi:10.1016/j.ydbio.2016.04.016

Wang, X., Chan, A. K. K., Sham, M. H., Burns, A. J. and Chan, W. Y. (2011). Analysis of the sacral neural crest cell contribution to the hindgut enteric nervous system in the mouse embryo. *Gastroenterology* **141**, 992-1002.e6. doi:10.1053/j.gastro.2011.06.002

Weskamp, G. and Reichardt, L. F. (1991). Evidence that biological activity of NGF is mediated through a novel subclass of high affinity receptors. *Neuron* **6**, 649-663. doi:10.1016/0896-6273(91)90067-A

Yahya, I., Böing, M., Brand-Saberi, B. and Morosan-Puopolo, G. (2021). How to distinguish between different cell lineages sharing common markers using combinations of double *in-situ*-hybridization and immunostaining in avian embryos: CXCR4-positive mesodermal and neural crest-derived cells. *Histochem. Cell Biol.* **155**, 145-155. doi:10.1007/s00418-020-01920-7

Yntema, C. L. and Hammond, W. S. (1954). The origin of intrinsic ganglia of trunk viscera from vagal neural crest in the chick embryo. *J. Comp. Neurol.* **101**, 515-541. doi:10.1002/cne.901010212

Young, H. M., Turner, K. N. and Bergner, A. J. (2005). The location and phenotype of proliferating neural-crest-derived cells in the developing mouse gut. *Cell Tissue Res.* **320**, 1-9. doi:10.1007/s00441-004-1057-5

Yusuf, F., Rehimi, R., Dai, F. and Brand-Saberi, B. (2005). Expression of chemokine receptor CXCR4 during chick embryo development. *Anat. Embryol.* **210**, 35-41. doi:10.1007/s00429-005-0013-9

Zou, Y. R., Kottmann, A. H., Kuroda, M., Taniuchi, I. and Littman, D. R. (1998). Function of the chemokine receptor CXCR4 in haematopoiesis and in cerebellar development. *Nature* **393**, 595-599. doi:10.1038/31269